iScience

CellPress
OPEN ACCESS

Review

Flexible pressure sensors via engineering microstructures for wearable human-machine interaction and health monitoring applications

Xihua Cui,[1] Fengli Huang,[2] Xianchao Zhang,[2] Pingan Song,[3,4,*] Hua Zheng,[5,*] Venkata Chevali,[3] Hao Wang,[3] and Zhiguang Xu[1,*]

SUMMARY

Flexible pressure sensors capable of transducing pressure stimuli into electrical signals have drawn extensive attention owing to their potential applications for human-machine interaction and healthcare monitoring. To meet these application demands, engineering microstructures in the pressure sensors are an efficient way to improve key sensing performances, such as sensitivity, linear sensing range, response time, hysteresis, and durability. In this review, we provide an overview of the recent advances in the fabrication and application of high-performance flexible pressure sensors via engineering microstructures. The implementation mechanisms and fabrication strategies of microstructures including micropatterned, porous, fiber-network, and multiple microstructures are systematically summarized. The applications of flexible pressure sensors with microstructures in the fields of wearable human-machine interaction, and *ex vivo* and *in vivo* healthcare monitoring are comprehensively discussed. Finally, the outlook and challenges in the future improvement of flexible pressure sensors toward practical applications are presented.

INTRODUCTION

Rapid developments in the fields of wearable human-machine interaction and healthcare monitoring with the assistance of big data, artificial intelligence, and the Internet of Things have greatly changed the ways of life and entertainment for people (Chen et al., 2021b; Lee and Ahn, 2020; Tan et al., 2020). For example, human-machine interaction technology allows people to communicate or control machines via tactile sensation (Pyo et al., 2021). In particular, wearable human-machine interaction technology provides tactile perception and physical comfort for the operator, demonstrating potential for application in both virtual and augmented reality (VR/AR) communication (Yin et al., 2021a, 2021b). Additionally, wearable healthcare monitoring devices attached to the human body can capture different physiological signals in real time for early detection and diagnosis of health conditions (Gao et al., 2019; Li et al., 2020a). In these wearable applications, flexible electronics play a core role in the efficient integration of people, machines, and their environment (Chen et al., 2019a). Compared with the conventional rigid silicon-based electronics, flexible electronics show advantages of withstanding various deformations such as tension, compression, bending, and torsion (Chen et al., 2020a; Cui et al., 2021; Li et al., 2021a). As a member of flexible electronic family, flexible pressure sensors can transduce external pressure from compression into electrical signals (resistance, capacitance, voltage, and current), and bear the potential for applications in wearable human-machine interaction and health monitoring (Chen et al., 2021c; He et al., 2021).

The sensing mechanisms of pressure sensors include piezoresistivity, capacitance, piezoelectricity, and triboelectricity (Niu et al., 2021). The schematic illustrations of these four sensing mechanisms are shown in Figure 1. The basic principle of piezoresistive pressure sensors is based on the resistance variation resulting from the change in the conductive path under pressure (Fu et al., 2021; Han et al., 2019b). The working mechanism of capacitive pressure sensors is the transduction of external pressure stimuli into a change in the capacitance of a parallel plate capacitor (Zhang et al., 2021b). For piezoelectric pressure sensors, the working principle is the separation of electric dipole moments resulting from the deformation of piezoelectric crystals under pressure, generating electrical signals (Guo et al., 2018; Pan and Lee, 2021). In addition, triboelectricity is another transduction method for pressure sensing, which refers to the generation of

[1]China-Australia Institute for Advanced Materials and Manufacturing, Jiaxing University, Jiaxing 314001, China

[2]College of Information Science and Engineering, Key Laboratory of Medical Electronics and Digital Health of Zhejiang Province, Engineering Research Center of Intelligent Human Health Situation Awareness of Zhejiang Province, Jiaxing University, Jiaxing 314001, China

[3]Centre for Future Materials, University of Southern Queensland, Springfield Central 4300, Australia

[4]School of Agriculture and Environmental Science, University of Southern Queensland, Springfield Central 4300, Australia

[5]School of Architecture and Energy Engineering, Wenzhou University of Technology, 1 Jingguan Road, Wenzhou University Town, Wenzhou 325035, China

*Correspondence: pingansong@gmail.com, pingan.song@usq.edu.au (P.S.), huazheng@wzu.edu.cn (H.Z.), zhiguang.xu@zjxu.edu.cn (Z.X.)

https://doi.org/10.1016/j.isci.2022.104148

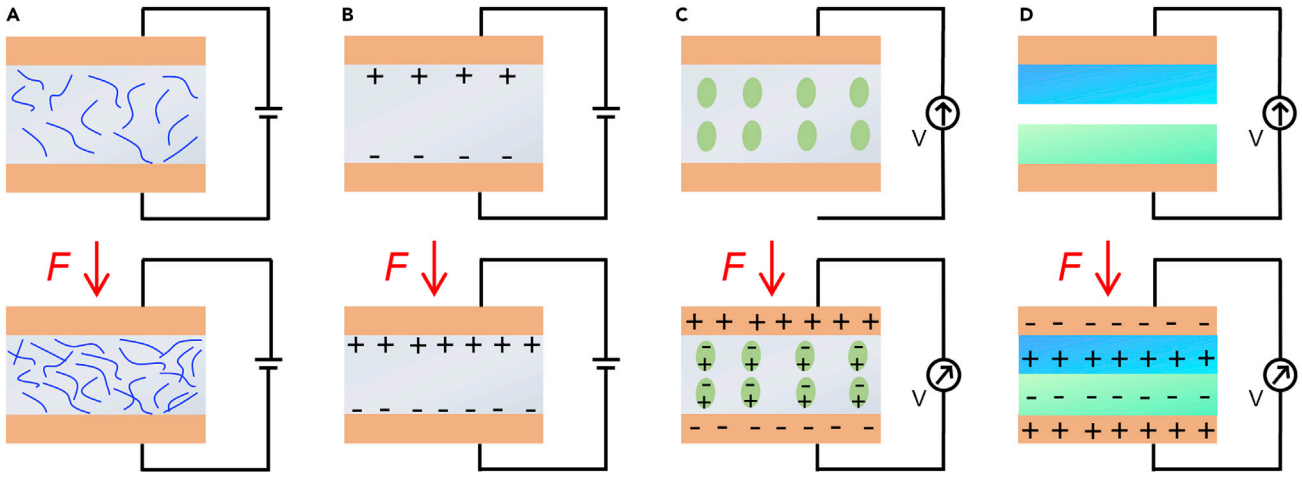

Figure 1. Schematic illustrations of sensing mechanisms of pressure sensors

(A) Piezoresistivity.

(B) Capacitance.

(C) Piezoelectricity.

(D) Triboelectricity.

different current or voltage signals under different pressures by triboelectrification and electrostatic induction (Luo et al., 2021). The piezoresistive and capacitive pressure sensors both require external batteries to supply power for the sensors (Amit et al., 2020; Sun et al., 2019; Zhou et al., 2020b). The piezoelectric and triboelectric pressure sensors can generate self-power, but they can only detect dynamic pressures rather than static pressures because they can only generate impulsive signals (Pyo et al., 2021).

To meet the demands of obtaining precise information in these wearable applications, the flexible pressure sensors are expected to meet key performance parameters, such as sensitivity, linear sensing range, response time, hysteresis, and durability (Liu et al., 2020b; Pyo et al., 2021; Zheng et al., 2020). Sensitivity is critical for sensing pressure, determining low detection limit, distinguishing subtle pressure, and measuring accuracy. Specifically, the sensitivity of a pressure sensor is defined as $S = (\Delta X/X_0)/P$, where ΔX *and* X_0 denote the change in the output electrical signal (resistance, capacitance, voltage, and current) and the initial signal, and P is the input external pressure (Ruth et al., 2020). The linear sensing range is also an important parameter for pressure sensors, which ensures high-pressure resolution of the sensors over a wide pressure range, and reduces the complexity of data processing (He et al., 2020a). It should be noted that many pressure sensors experience a tradeoff between sensitivity and the linear sensing range, which severely limits their applications. Specifically, sensors with high sensitivity are usually realized in a limited sensing range, whereas sensors that can detect a broad range of pressures suffer from nonlinearity and unstable responses in the low-pressure ranges (Xiang et al., 2021; Zhu et al., 2020). Furthermore, the response time is defined as the time for pressure sensors to obtain a stable output signal in response to pressure stimulus, which is crucial for high-frequency signal detecting (Chen et al., 2021a; Tang et al., 2021). Hysteresis is used to measure the difference in the output signal versus pressure curve under loading and unloading of pressure (Yao et al., 2020). The drawback of high hysteresis exists in almost all flexible pressure sensors due to the viscoelasticity of the flexible materials, which should be minimized in practical applications (Li et al., 2020a). Durability is the parameter defined as the resistance of the signal against repeated loading and unloading processes, which represents the long-time sensing ability (Yin et al., 2021c).

Generally, flexible pressure sensors comprise of multiple layers, including top and bottom electrode layers, and at least one intermediate sensing layer (piezoresistive, capacitive, piezoelectric, or triboelectric layer) (Ruth et al., 2020). Correspondingly, flexible pressure sensors are made of three kinds of materials: substrate materials, electrode materials, and active sensing materials. The performance of flexible pressure sensors is dictated by both the constituent material and structure. To improve the comprehensive sensing performance, a common strategy is to use engineering microstructures in the sensing or electrode layers of pressure sensors (He et al., 2021; Liu et al., 2018; Wang et al., 2021a). For example, the piezoresistive pressure sensors with microstructures can significantly increase the contact area and conductive path under

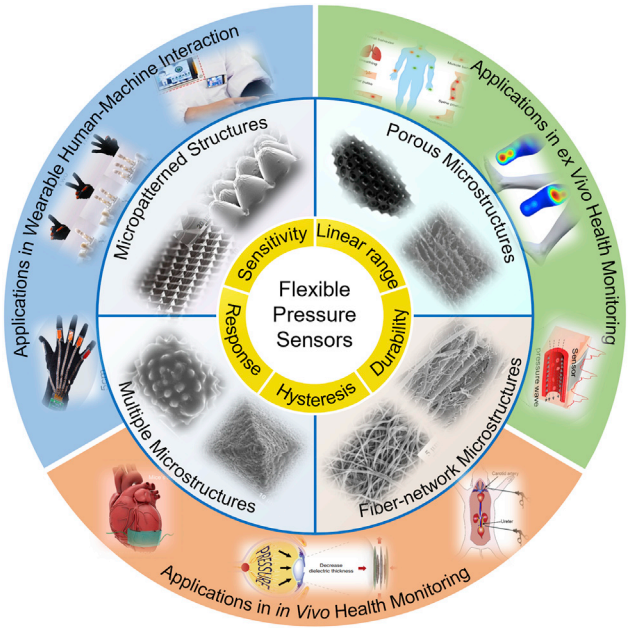

Figure 2. Overview of the review

Flexible pressure sensors with microstructures and the potential applications in wearable human-machine interaction, *ex vivo* health monitoring, and *in vivo* health monitoring. Adapted with permission (Kim et al., 2017). Copyright 2017, Nature Publishing Group (Yang et al., 2019b). Copyright 2019, American Chemical Society (Yang et al., 2021b). Copyright 2021, American Chemical Society (Chen et al., 2020c). Copyright 2020, Elsevier Ltd (Zhong et al., 2021). Copyright 2021, Elsevier Ltd (Chao et al., 2021). Copyright 2021, American Chemical Society (Kim et al., 2019). Copyright 2019, American Chemical Society (Wang et al., 2021b). Copyright 2021, Elsevier Ltd (Wang et al., 2021d). Copyright 2021, American Chemical Society (Zhao et al., 2020). Copyright 2020, American Chemical Society (Zhao et al., 2021b). Copyright 2021, Elsevier Ltd (Liu et al., 2021). Copyright 2021, Wiley-VCH GmbH (Zou et al., 2019). Copyright 2019, Wiley-VCH Verlag GmbH & Co. KGaA, Weinheim (Yao et al., 2020). Copyright 2020, National Academy of Sciences (Wu et al., 2020a). Copyright 2020, American Chemical Society.

subtle pressure due to the stress concentration effect, thus effectively improving the sensitivity of the sensors (Chen et al., 2020d; Guan et al., 2020; Peng et al., 2018). By introducing micropatterns into the sensing or electrode layers, the compressibility and the effective dielectric constant change can be improved, leading to larger capacitance variation of the capacitive pressure sensors (Zhang et al., 2021b). For the piezoelectric pressure sensors with microstructures, due to the enhanced compressibility and the strain confinement effect, microstructures deform more under a given pressure than the planar film structure, which causes a larger output voltage (Chen et al., 2020d). For the triboelectric pressure sensors, engineering microstructures in the sensing layer can greatly improve the effective contact area, provide numerous active sites for the transfer of electrostatic charges, and increase the friction charge density of the friction surface, leading to the enhancement of the triboelectric effects (Zhang et al., 2019a). In the past decade, engineering microstructures have been established as highly effective performance improvers for pressure sensors (Kong et al., 2020; Li et al., 2021b; Zhang et al., 2020b). A divergent range of microstructures with varied implementation mechanisms have been explored intensively as a result.

Until now, most review papers on flexible pressure sensors have mainly focused on the sensing mechanisms and emerging materials for pressure sensors including substrate materials and sensing active materials, while others have paid attention to novel applications of pressure sensors (Li et al., 2020a; Yin et al., 2021a; Zheng et al., 2020). Only recently, Ruth et al. systematically summarized the progress of employing geometric microengineering design to improve the performance of capacitive, resistive, piezoelectric, and triboelectric pressure sensors (Ruth et al., 2020). In this review, we summarize the most recent advances in the field of flexible pressure sensors with novel and comprehensive microstructures, which offer renewed inspiration for improving sensing performance by engineering microstructures. Figure 2 provides an overview of this article. We first review the engineered microstructures for high-performance flexible pressure sensors, including micropatterned, porous, fiber-network, and multiple microstructures. In each section,

the implementation mechanisms and fabrication strategies to realize corresponding microstructures are systematically summarized. Subsequently, we introduce major advances and applications of flexible pressure sensors in wearable human-machine interaction, *ex vivo*, and *in vivo* healthcare monitoring. Finally, the future challenges of flexible pressure sensors with microstructures are briefly discussed.

MICROSTRUCTURES AND FABRICATION STRATEGIES FOR HIGH-PERFORMANCE FLEXIBLE PRESSURE SENSORS

High-performance flexible pressure sensors are highly desired to meet the growing demand of precisely obtaining external force signals in those wearable applications. In recent years, sensing performances have been effectively improved by introducing microstructures into the pressure sensors (Niu et al., 2021). In this section, we systematically introduce four types of microstructures including micropatterned, porous, fiber-network, and multiple microstructures. We explain the corresponding implementation mechanism and elaborate on the influence of microstructure on sensing performance and present the fabrication strategies to realize each microstructure. Moreover, we summarize and compare the sensing performance of the flexible pressure sensors with the four types of microstructures in Table 1, intuitively reflecting on the role of microstructures.

Micropatterned structures

Micropatterned structures refer to the formation of arrays with micron-sized patterns throughout the sensor, which are the most commonly used microstructures to improve the performance of pressure sensors (Chen et al., 2017, 2020b; He et al., 2021). The shapes for micropatterned structures include both irregular shapes and regular shapes such as pillars, pyramids, and domes (Chen et al., 2019b; Choong et al., 2014; Tang et al., 2019). The fundamental implementation mechanism for micropatterned structures lies in the enhanced compressibility and the stress concentration effect (Zhao et al., 2020). The main reason for the effectiveness of micropatterning is the resultant decrease in elastic resistance and increase in compressibility due to the introduction of an air gap that causes an increase in pressure response range of the sensor. Another reason is the geometry of micropatterned structures causing stress to be concentrated at the tip of the structure (He et al., 2020b). Thus, under a given applied pressure, this large stress concentration results in significant changes in contact area compared to a planar structure (Li et al., 2019). For example, Ma et al. constructed flexible pressure sensors by laminating a thin layer of conductive polydimethylsiloxane/carbon nanotube (PDMS/CNT) film with regular micropyramidal patterns on the interdigitated electrodes as shown in Figure 3A (Ma et al., 2020). Their numerical simulations show that increasing applied pressure reduces the pyramid height and results in a large increase in the contact area, which leads to a decrease in the contact resistance and a corresponding increase in current flow through the sensor. Moreover, it has been found that the pressure sensing performance of the sensor can be readily tuned by the spatial arrangement of the pyramids. When the ratio between the spacing and the pyramidal base length is 1:1, the optimal pressure sensing performance can be achieved with high sensitivity in both low-pressure (<10 kPa) and medium-pressure (10–100 kPa) regions, fast response time, linear response, and low hysteresis in the medium-pressure regime.

As well as the regular micropattern structures, irregular micropattern structures are also employed to improve the performance of pressure sensors. Bai et al. proposed an iontronic flexible pressure sensor using polyvinyl alcohol (PVA)/H_3PO_4 film with graded intrafillable architecture as the dielectric layer (Bai et al., 2020). The PVA/H_3PO_4 film was fabricated by demolding from sandpaper, featuring undercuts and grooves that accommodate deformed surface microstructures, effectively enhancing the structural compressibility and the pressure-response range. The prepared pressure sensor exhibited an unprecedentedly high sensitivity (220 kPa^{-1}) over a broad pressure regime (0.08 Pa–360 kPa), and an ultrahigh-pressure resolution (18 Pa or 0.0056%) over the full pressure range (Figure 3B).

For the above-mentioned flexible pressure sensors with single-layer micropatterned structures, the deformation of the microstructures under pressure quickly reaches its saturation (i.e., the microstructure is flattened) due to the micro size. Thus the compressibility of the sensing layer and the sensing range of the sensors is still limited. To meet the requirements of high sensitivity in a wide sensing range, one of the methods is constructing a double-layer or multilayer micropatterned structure. For a double-layer micropatterned structure, the interlocked form inspired by the interlocked microridges between the dermis and epidermis of human skin is widely implemented. For instance, Zhang et al. fabricated large-area uniform micropatterns with quasi-hemispherical shapes with the facile method of hot-air-gun assisted

Table 1. Summary of the sensing performance of the flexible pressure sensors via engineering various microstructures

Microstructure types	Materials	Maximum sensitivity (kPa^{-1})	Linear sensing range (kPa)	Response time (ms)	Durability (cycles)	Ref
Micropatterned structure	CNPs/CFs/PDMS	26.6	0.02–600	40	5,000	(Zhong et al., 2021)
	TPU/SWCNTs	0.02	0.055–254.8	46	20,000	(Zhang et al., 2021a)
	PU/AgNW	4.169	0.02–10.3	20	2,300	(Zhu et al., 2020)
	PDMS/CNT	20.9	0.0074–1000	23	10,000	(Wu et al., 2020b)
	TPV matrix/Ni	10^6	0.001–500	50	500	(Tian et al., 2020)
	PDMS/PEDOT: PSS/PUD	3.8×10^5	0.000025–100	0.016	8,000	(Lee et al., 2021b)
	Graphene/PVDF	25.9	0.01–1400	3.5	10,000	(Kong et al., 2020)
	PDMS/MXene	151.4	0.0044–15	130	10,000	(Cheng et al., 2020)
	rGO/PDMS	55	0.004–400	30	9,000	(Zhang et al., 2019b)
	Electrodes: PDMS/PPy ITO Dielectric layer: Ionic gel	26.6	0.644–26.6	48	8,000	(Zheng et al., 2021)
	Electrodes: PI/Au, PDMS/Au Dielectric layer: Ionic gel	33.16	12–176	9	6,000	(Lu et al., 2021)
	Electrodes: PDMS-Au Dielectric layer: PVDF	30.2	0–130	25	100,000	(Xiong et al., 2020a)
Porous microstructure	TPU/CNTs	1.02	0.0007–160	65	60,000	(Yin et al., 2021c)
	TPU/CB	1.12	0.02–1200	15	10,000	(Guan et al., 2020)
	TPU/Ag	5.54	0.01–800	20	10,000	(Wang et al., 2019)
	MXene/Tissue paper	3.81	0.0102–30	11	10,000	(Guo et al., 2019)
	PGS	0.18	0–6	50	10,000	(Sencadas et al., 2021)
	PINF/MXene aerogel	0.14	0–80	220	1,000	(Liu et al., 2021)
	CNT/PDMS sponge	0.02	0.01–1200	–	10,000	(Kim et al., 2019)
	Electrodes: CNTs/PDMS Dielectric layer: PDMS	0.059	0–100	80	1,000	(Jung et al., 2021)
Fiber-network microstructure	MXene/PAN	104.0	0.2–7.7	30	10,000	(Fu et al., 2021)
	Ag NWs/graphene/PANFs	134	0.0037–75	20	8,000	(Li et al., 2020b)
	MXene/SF	298.4	0–39.3	7	10,000	(Chao et al., 2021)
	PA 66/Au/PAN	0.217	0–3	–	–	(Peng et al., 2021)
	Electrodes: Au/M-PDMS Dielectric layer: Ionic nanofibrous membrane	5.5	0–250	70.4	20,000	(Sharma et al., 2021)
	Electrodes: CPI Dielectric layer: Fabric-IL	13.5	0.0075–175	30	5,000	(Lin et al., 2020)
	Electrodes: PI/AgNWs Dielectric layer: TiO_2 nanofiber	4.4	0.0008–120	16	50,000	(Fu et al., 2020)
Multiple microstructure	MHA@Cu mesh	307	1–20	0.63	2,700	(Zhou et al., 2020a)
	MWCNT/PDMS	4.60	0–218	31	9,000	(Zhao et al., 2020)
	ZnOEP/CNT/PDMS	39.4	0–100	3	5,000	(Zhang et al., 2020b)
	PDMS/CB/PI/LIG	43	0.4–13.6	40	1,800	(Yi et al., 2020)
	Pt/PDMS	10^7	0–20	2.5	10,000	(Yao et al., 2020)
	CNT/PDMS	5.6	0–600	60	33,000	(Bae et al., 2016)
	Poly(PDES)	348.28	0.0006–2000	20	45,000	(Cai et al., 2021)
	Electrodes: ITO/PET Dielectric layer: Porous pyramid dielectric layer	44.5	0–35	50	5,000	(Yang et al., 2019b)

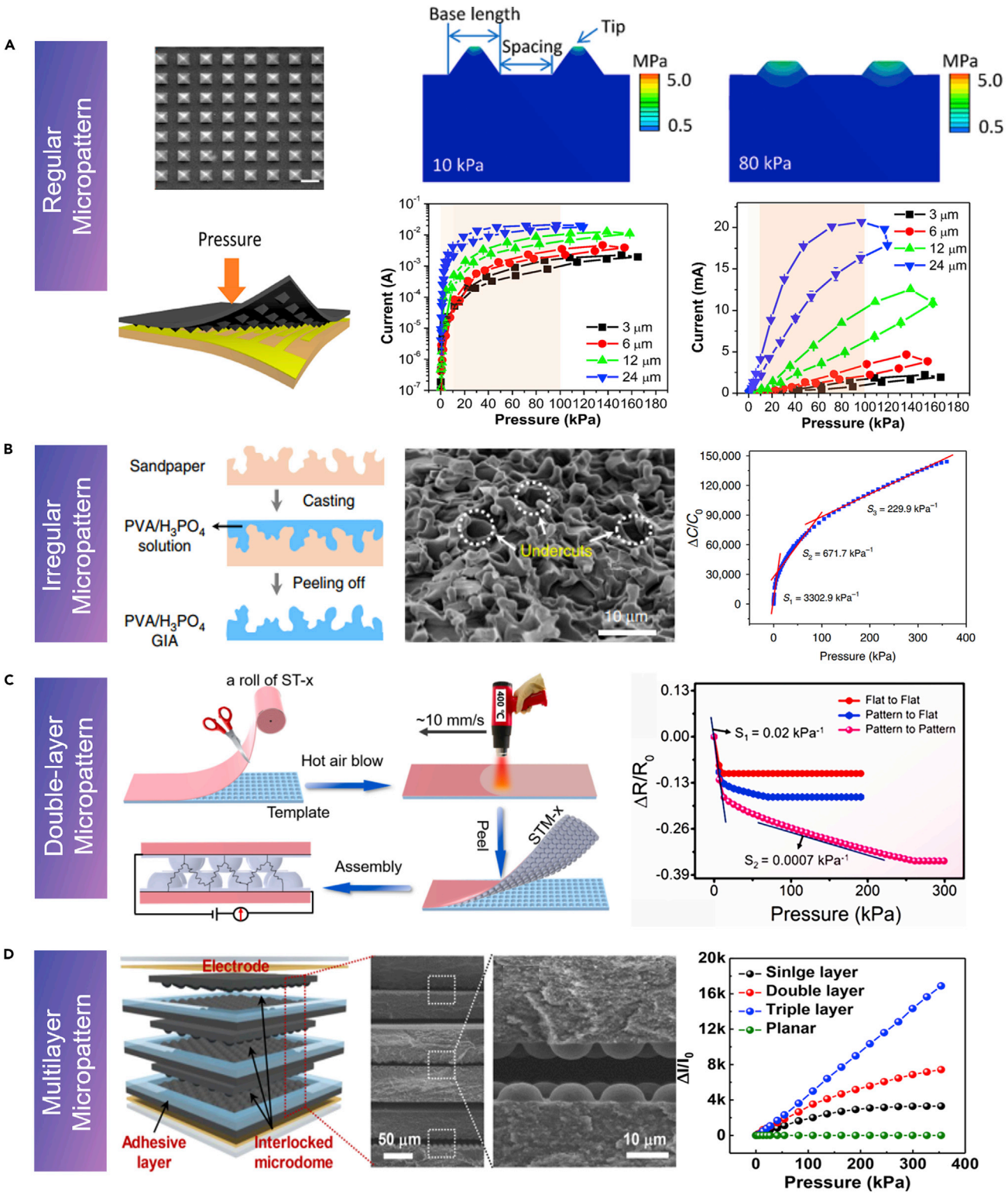

Figure 3. Flexible pressure sensors with micropatterned structures

(A) SEM image of the PDMS/CNT layer with micropyramidal structures, mechanical simulation of cross-sectional views of deformation and stress intensity distribution of the micropyramidal film, schematic illustration, and the pressure responses of the piezoresistive pressure sensors with different spacing. Adapted with permission (Ma et al., 2020). Copyright 2020, American Chemical Society.

Figure 3. *Continued*

(B) Schematic illustration of the preparation of PVA/H_3PO_4 film with graded intrafillable architecture, the SEM image of the film, and the change of capacitance over the pressure range up to 360 kPa. Adapted with permission (Bai et al., 2020). Copyright 2020, Nature Publishing Group.

(C) Schematic illustration of the fabrication process of pressure sensor with interlocked quasi-hemisphere array and the relative resistance change of the pressure sensor versus pressure. Adapted with permission (Zhang et al., 2021a). Copyright 2020, Elsevier Ltd.

(D) Schematic of the piezoresistive pressure sensor with multilayer interlocked microdomes, and the response curves of the pressure sensor with multilayer geometry with different numbers of stacked layers and planar geometry to the applied pressure. Adapted with permission (Lee et al., 2018). Copyright 2018, American Chemical Society.

preparation (Zhang et al., 2021a). Then, the interlocked piezoresistive pressure sensor is constructed by face-to-face assembly of the double-layer micropatterns (Figure 3C). As a result, the as-prepared pressure sensor exhibited improved sensing performances, such as very fast response time (<46 ms), wide working range (0.055–254.8 kPa), and excellent durability (>20000 cycles) due to the interlocked microstructures. In addition, multilayer micropatterned structures are a more efficient way to increase the compressibility and contact area, thus endowing pressure sensors with high sensitivity over a broad linear range. For example, a piezoresistive pressure sensor with multilayer interlocked microdomes was proposed by Ko and co-workers (Figure 3D) to provide high sensitivity (47.7 kPa^{-1}), ultrawide linear sensing range of 0.0013–353 kPa with fast response time (20 ms), and high reliability over 5000 repetitive cycles (Lee et al., 2018).

With the rapid development of high-performance flexible pressure sensors, many strategies for fabricating micropattern arrays have emerged. The most common strategy is the template method, which possesses the advantages of low cost, mass production, and repeated use. Specifically, the polymer (e.g., PDMS, Ecoflex, and thermoplastic polyurethane) liquid is poured into the template, cured, and peeled off from the template to obtain the micropattern arrays (Ma et al., 2020). Among these templates, the silicon template is widely used to design microstructures with the desired size and shape to match the experimental requirements. Moreover, the patterns created from silicon templates are regular and uniform, which is critical for fabricating high-performance sensors with uniform microstructures. For example, Ji et al. used a silicon template with through-hole arrays drilled via laser etching (Figure 4A). Then, a PDMS film with predefined thickness was attached to the silicon template with vacuum on underneath, producing a curved depression array. The curved depression array was used as a template to prepare a dome array or hierarchical pillar—dome array structure as the sensing element, contributing to excellent sensitivity (128.29 kPa^{-1}, 0–200 Pa) and controllable detection range (0–80 kPa) (Ji et al., 2019). Choong et al. replicated a PDMS substrate with micropyramids from a silicon mold, and then grafted a sub-micrometer-thick conductive composite on the PDMS substrate to obtain a micropyramidal electrode (Figure 4B). The micropyramidal electrode was then assembled with a counter electrode to construct a piezoresistive pressure sensor with a uniform micropatterned structure (Choong et al., 2014).

The silicon template method possesses significant advantages in the fabrication of micropatterned structures, while it is restricted by its complex processing and high cost. Recently, researchers have created many unique micropatterned structures using naturally occurring mold materials such as rose petals and lotus leaves (Shi et al., 2018). For example, Yang et al. were first to experiment with PVA solution, where they poured this solution onto rose petals, followed by thorough drying (Yang et al., 2021b). As a result, an inverse petal structure with micropattern array was obtained after detaching the film from the rose petal. Afterwards, the PDMS precursor was spin coated on the PVA film and completely cured, and a microdome-structured PDMS film was obtained by dissolving the PVA film. Finally, gold was sputtered on the surface of the micropatterned PDMS film layer to be used as an electrode (Figure 4C). Alternatively, micropatterning can also be achieved by using commercially available mold materials, resembling the aforementioned sandpaper in Figure 2B (Bai et al., 2020). Recently, Wu et al. hot pressed a piece of stainless-steel screen mesh into the surface of a polystyrene (PS) sheet (Wu et al., 2020b). After cooling, the screen mesh was peeled off from the PS sheet, leaving an inverse mesh microstructure on the PS template. Then, a conductive CNT layer was uniformly spray coated on the inverse microstructured PS template, followed by casting a PDMS precursor. After PDMS was cured, the conductive PDMS/CNT film with large-area micropatterned structures was peeled off, serving as sensing layer for the piezoresistive pressure sensors (Figure 4D). Although natural and commercially available molds simplify the fabrication process, the uniformity and controllability of micropatterned structures are albeit reduced.

In addition to the template method, the micropatterned structures can also be constructed by directly structuring the flexible film without using a mold (Wu et al., 2021). One way of achieving this micropattern

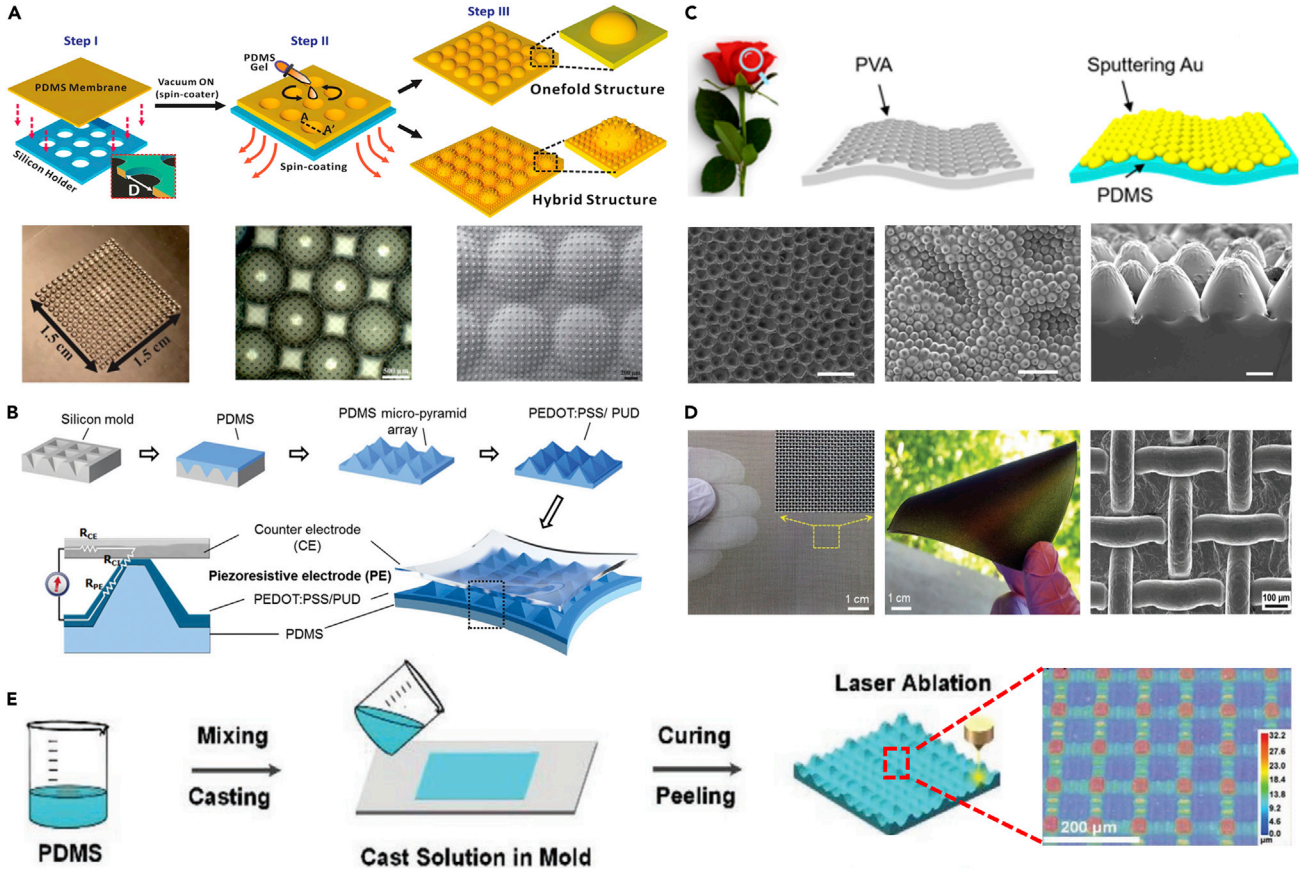

Figure 4. Fabrication strategies of micropatterned structures

(A) Schematic illustration of the fabrication process of mesodome and micropillar structures through silicon templates with through-hole arrays and images of the structures. Adapted with permission (Ji et al., 2019). Copyright 2019, American Chemical Society.

(B) Schematic illustration of the fabrication process of PDMS film with micropyramid arrays by the silicon mold and the structure of the piezoresistive pressure sensor. Adapted with permission (Choong et al., 2014). Copyright 2014, Wiley-VCH Verlag GmbH & Co. KGaA, Weinheim.

(C) Diagram illustrating the fabrication procedure of the microdome structure inspired by rose petals and SEM images of inverse petal structure PVA film and the microdome-structured PDMS film. Adapted with permission (Yang et al., 2021b). Copyright 2021, American Chemical Society.

(D) Photographs of the stainless-steel screen mesh used as the mold, picture of the as-prepared conductive PDMS/CNT film with micropatterned structure, and SEM image of the PDMS/CNT microstructure. Adapted with permission (Wu et al., 2020b). Copyright 2020, Wiley-VCH Verlag GmbH & Co. KGaA, Weinheim.

(E) The fabrication process of flexible pressure sensor based on controllable hierarchical micropatterned structures by laser scribing and the 3D morphology of laser-scribed PDMS surface. Adapted with permission (Du et al., 2021). Copyright 2021, Wiley-VCH GmbH.

is by laser scribing. For instance, Du et al. ablated flat PDMS film using a commercial femtosecond laser to directly obtain a hierarchical micropatterned structure (Figure 4E). Specifically, the hierarchical microstructure was obtained by adjusting the laser power and the scribing pattern (Du et al., 2021). Although the directly structuring method possesses simplified fabrication processes, the authors note distinct differences between preparation from diverse batches.

Porous microstructures

Micropatterned structures are usually constructed on the surface of a flexible substrate, which could sense subtle external mechanical stimuli. But the limited deformation of micropatterns leads to saturation under pressure, causing failure in sensing high pressures. Three-dimensional porous materials possess remarkable mechanical compressibility with abundant porous networks that can interconnect under high pressure, thus becoming promising candidates for pressure sensors with a broad sensing range (Dai et al., 2021; Ding et al., 2019; Wang et al., 2021c).

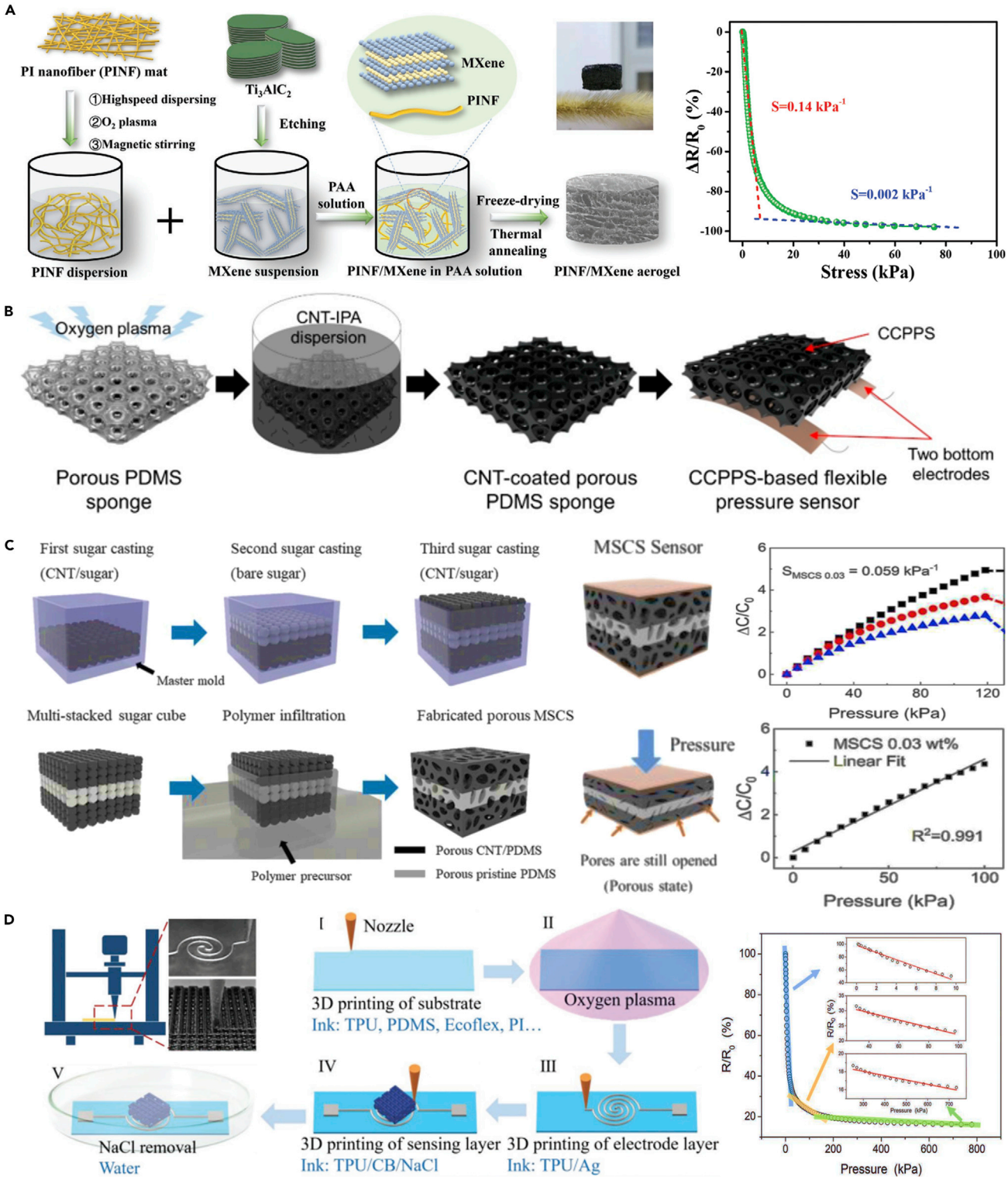

Figure 5. Flexible pressure sensors with porous microstructures

(A) Schematic diagram for the preparation process of PINF/MXene composite aerogel and relative resistance change of PINF/MXene composite aerogel as a function of pressure. Adapted with permission (Liu et al., 2021). Copyright 2021, Wiley-VCH GmbH.

(B) Schematic illustration of the fabrication procedure of the pressure sensor based on a CNT network-coated porous PDMS sponge. Adapted with permission (Kim et al., 2019). Copyright 2019, American Chemical Society.

Figure 5. *Continued*
(C) Schematic of the fabrication procedure of capacitive pressure sensor with three-dimensional and porous structure by removing sugar template and pressure-response curves for the sensor. Adapted with permission (Jung et al., 2021). Copyright 2021, American Chemical Society.
(D) Schematic of the fabrication procedure of piezoresistive pressure sensor with multilayer porous structure combining 3D printing and removing NaCl template. Adapted with permission (Wang et al., 2019). Copyright 2018, Wiley-VCH Verlag GmbH & Co. KGaA, Weinheim.

Aerogel is one such porous material with a nanoscale structure, which has been widely studied recently (Bi et al., 2020). Owing to its high porosity, excellent compressibility, and electrical conductivity, the ultralight, compressible aerogel materials are recognized for their broad application prospects in the field of flexible pressure sensors (Min et al., 2021). Liu et al. fabricated conductive polyimide nanofiber (PINF)/Mxene composite aerogel with a special "layer-strut" bracing hierarchical cellular structure through a simple freeze-drying and thermal imidization process (Figure 5A). Upon pressing the composite aerogel, the contact area of its struts sharply increased due to the deformation of a porous structure, leading to changes in electrical resistance. Meanwhile, the elasticity ensures the resistance recovery after the pressure is released, endowing it with favorable cyclic stability. Therefore, the developed composite aerogel was used as a piezoresistive sensor with an outstanding sensing capacity up to 90% strain (corresponding 85.21 kPa), ultralow detection limit of 0.5% strain (corresponding 0.01 kPa), robust fatigue resistance over 1000 cycles, excellent piezoresistive stability, and reproductivity in extremely harsh environments (Liu et al., 2021).

It should be noted that the fabrication process of aerogel-based pressure sensors is complex and involves high cost, which impedes their large-area production and thereby their practical applications in sensors. One simple way of fabricating pressure sensors with porous microstructures is to start with an already porous material such as sponge as the substrate (Xiong et al., 2020b). The conductive porous sponge-like sensing layers are typically fabricated by a coating process or a direct synthesis of the conductive nanomaterials such as metal nanowires, graphene, and CNTs on the backbones (Jang et al., 2021). For example, Kim et al. fabricated a flexible piezoresistive pressure sensor based on a CNT-coated porous PDMS sponge, integrated with two bottom electrodes (Figure 5B). The presence of micropores provided high compressibility and large changes in contact between the conductive CNT networks, endowing the pressure sensor with ultrawide pressure sensing range (10 Pa–1.2 MPa), favorable sensitivity (0.01–0.02 kPa^{-1}), and good linearity ($R^2 \sim 0.98$) (Kim et al., 2019). Utilizing an already porous material as the substrate realizes the large-scale fabrication of pressure sensors with porous microstructures. However, the challenge is the lack of control of pore size and structure, which can influence the reproducibility and tunability of the structure and performance of the sensors.

Furthermore, the flexible pressure sensors with porous microstructures can also be fabricated with the assistance of a porogen, such as NaCl or sugar particle as the sacrificial template (Kim et al., 2019; Yang et al., 2020). One method is to coat conductive polymer composite precursor on a particular structure constructed by the sacrificial template, and then immerse it in the etching solution to remove the porogen after curing to sacrifice the template, thereby obtaining the porous conductive polymer composite with the desired structure. For example, Jung et al. uniformly mixed sugar with CNT and pure sugar, respectively (Jung et al., 2021). Then, the CNT/sugar, bare sugar, and CNT/sugar were stacked in sequence in the master mold, and treated in an oven to form a sugar cube (Figure 5C). Afterwards, the sugar cube was filled with PDMS precursor in a vacuum chamber and cured by heat. Finally, the porous multistacked composite structure was obtained by immersing the sugar cube in water to remove the sugar, which could be used as a capacitive pressure sensor. This multistacked structure efficiently distributes applied stress to each layer, thereby resulting in a wide pressure range and high linearity compared to a single-layer structure. The designed pressure sensor exhibited linear sensitivity (0.059 kPa^{-1}, R^2 = 0.991) in the medium-pressure range (10–100 kPa). Alternatively, a second strategy is to directly mix the sacrificial porogen and conductive nanomaterials with polymer, and dissolving the porogen in water to obtain a flexible pressure sensor with a porous microstructure. For instance, Wang et al. thoroughly mixed NaCl and carbon black (CB) with thermoplastic polyurethane (TPU) sol to obtain a conductive printable ink (Wang et al., 2019). Then, the three-dimensional multilayered structure was built via 3D printing. After removing the sacrificial template by dissolving NaCl in water, the piezoresistive pressure sensors with a hierarchically porous architecture were realized (Figure 5D). Benefiting from the hierarchically porous structure, this sensor exhibited a large measurement range (from 10 Pa to 800 kPa), limited cross-correlation, and excellent durability.

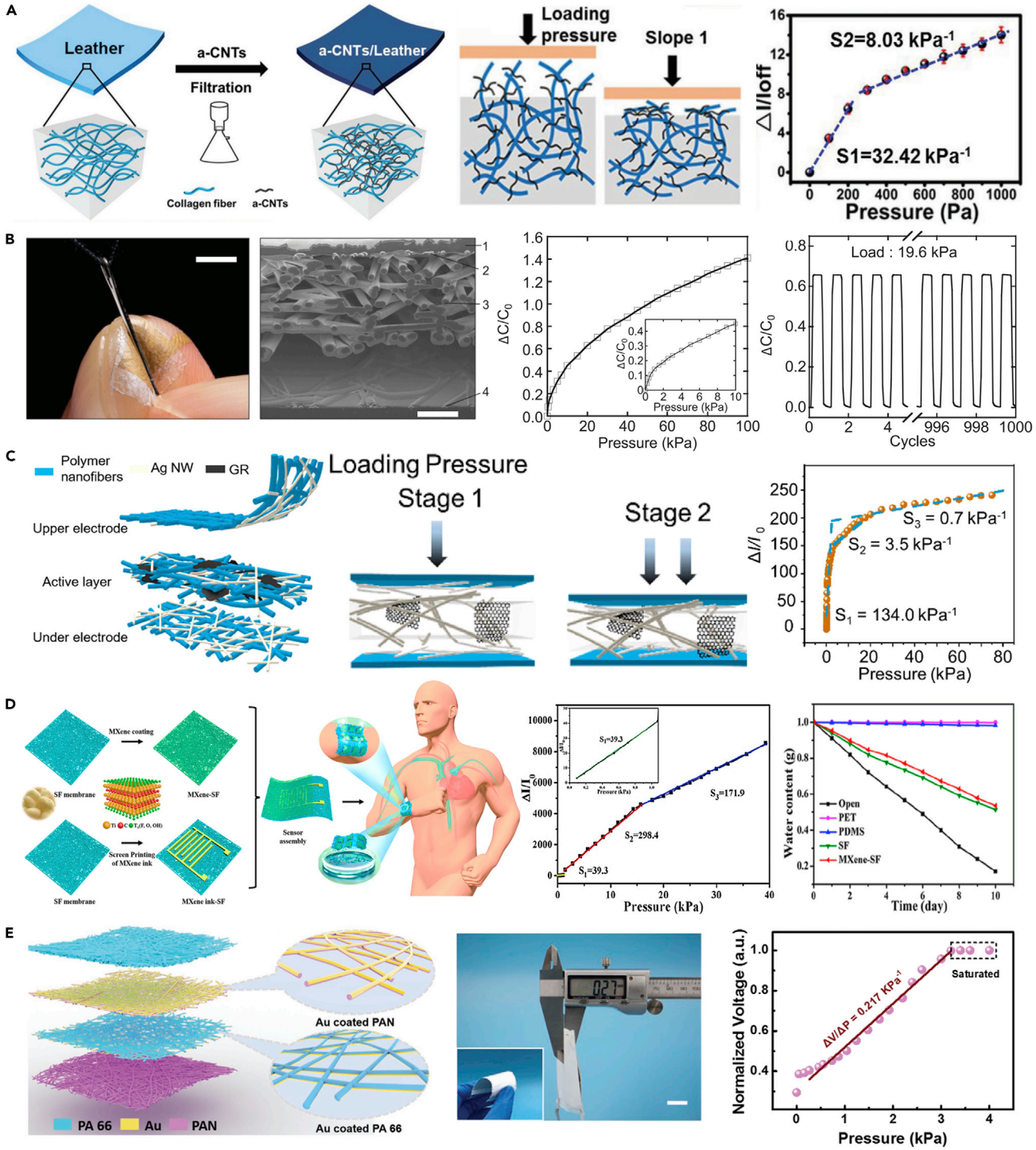

Figure 6. Flexible pressure sensors with fiber-network microstructures

(A) Schematic illustration of the fabrication process of conductive leather by filtrating a-CNTs through leather, the proposed pressure sensing mechanism, and the current responses of the sensor to various pressures. Adapted with permission (Zou et al., 2019). Copyright 2018, Wiley-VCH Verlag GmbH & Co. KGaA, Weinheim.

(B) Structure of the nanomesh pressure sensor, the relative capacitance change as a function of pressure applied to sensor, and the pressure sensitivity of the nanomesh sensor during 1000 cyclic pressure applications. Adapted with permission (Lee et al., 2020). Copyright 2020, American Association for the Advancement of Science.

Figure 6. *Continued*

(C) Schematic illustration presenting the structure of the Ag NWs/GR/PANF pressure sensor, the proposed pressure sensing mechanism, and the current response of the sensor versus applied pressure. Adapted with permission (Li et al., 2020b). Copyright 2020, American Chemical Society.

(D) Schematic diagram of the fabrication procedure of the breathable and degradable MXene/SF membrane-based pressure sensor, sensing sensitivity of the pressure sensor under the externally loaded pressure, and the breathability of the MXene/SF membrane compared with other flexible polymer films. Adapted with permission (Chao et al., 2021). Copyright 2021, American Chemical Society.

(E) Schematic illustration of the structure of the all-nanofiber TENG, photograph image of the all-nanofiber TENG with a total thickness of 270 μm, and normalized output voltage response to a wide range of pressures. Adapted with permission (Peng et al., 2021). Copyright 2021, Wiley-VCH GmbH.

Fiber-network microstructures

The porous microstructures can effectively broaden the sensing range, but the sensors suffer from low sensitivity in the low-pressure range and large residual deformation in repeated compression, which seriously restrict their applications (Zhang et al., 2020a). Recently, the flexible pressure sensors with fiber-network microstructures have attracted considerable attention from academia and industry (Guo et al., 2019; Han et al., 2019a; Peng et al., 2020). Fiber networks are full of microfibers that interlace with each other, forming abundant fibrous and hierarchical porous structures that can be sensitively compressed by pressure, which show great potential for the fabrication of flexible pressure sensors (Gong et al., 2020; Yang et al., 2019a). For example, Zou et al. reported a simple leather-based pressure sensor by merging the natural sophisticated structure and wearing comfort of leather (Zou et al., 2019). The pressure sensor was prepared by filtrating CNTs using leather as a filter, and then distributing CNTs inside the hierarchical structure of leather (Figure 6A). The leather naturally inherits a hierarchical fibrous structure such as a collagen fibril (nm), collagen fiber (μm), and leather (cm), which can be compressed by pressure. Because a hierarchical fibrous and porous structure constituted the leather, the sensor exhibited a high sensitivity of 32.42 kPa^{-1} when the pressure was lower than 200 Pa. Lee et al. developed ultrathin nanomesh capacitive pressure sensors with nanoporous structures that can attach directly to the skin without any noticeable effects on human sensation (Lee et al., 2020). The nanomesh pressure sensor consisted of four nanomesh layers, all of which were prepared by electrospinning (Figure 6B). The sensor showed high sensitivity of 0.141 kPa^{-1} in the low-pressure range (<1 kPa), 0.010 kPa^{-1} in the high-pressure range (>10 kPa), and good durability over 1000 cycles, capable of monitoring finger manipulation. Electrospinning particularly is an efficient method for fabricating flexible pressure sensors with fiber-network microstructures. For example, Li et al. prepared an ultrathin flexible piezoresistive pressure sensor with a hierarchical nanonetwork structure processed through electrospinning (Figure 6C). The hierarchical nanonetwork material comprised silver nanowires (Ag NWs), graphene (GR), and polyamide nanofibers (PANFs) (Li et al., 2020b). Linked to the hierarchical nanonetwork structure, the sensor exhibited a high sensitivity of 134 kPa^{-1} (0–1.5 kPa), low detection of 3.7 Pa, excellent durability (>8000 cycles), and a wide detection range (>75 kPa).

More importantly, the fiber network can be easily integrated with clothes and the breathability resulting from the porous structure guarantees wearing comfort (Cui et al., 2022; Lee et al., 2021a; Yu et al., 2021). Thus, the fiber-network microstructure is an ideal platform for the pressure sensors. Recently, Chao et al. fabricated MXene/protein-based pressure sensor with high flexibility, facile degradability, and breathability (Chao et al., 2021). Both the sensing layer and the electrode layer were based on silk fibroin nanofiber membranes that endowed the sensor with good biocompatibility and robust degradability (Figure 6D). The pressure sensor exhibited a wide sensing range up to 39.3 kPa, high sensitivity of 298.4 kPa^{-1} for 1.4–15.7, and 171.9 kPa^{-1} for 15.7–39.3 kPa, and fast response/recovery time of 7/16 ms, respectively. Moreover, the fibrous and porous structure of the pressure sensor engenders good breathability, desirable for compatibility between the human skin and the sensor. In addition, Peng et al. successfully developed a triboelectric nanogenerator (TENG)-based all-nanofiber thin e-skin through electrospinning method (Figure 6E). Owing to the numerous 3D micro-to-nano-nanofiber network structures, the all-nanofiber e-skin can not only harvest subtle vibration energy under low frequencies but also is responsive to tiny vibration energy with a high sensitivity of 0.217 kPa^{-1}. Furthermore, the e-skin possessed good breathability resulting from the numerous 3D hierarchical pores constructed by the multilayer stacking nanofiber networks, which is important for wearing comfort (Peng et al., 2021).

In brief, the fiber-network microstructures possess hierarchical porous structures constructed by the intertwining of fibers, which can be more readily compressed by pressure. Thus, the flexible pressure sensors with fiber-network microstructures exhibit a moderate linear sensing range and higher sensitivity than those comprised of porous microstructures. Moreover, the fiber network can be easily integrated with

fabrics and the breathability guarantees wearing comfort, demonstrating great potential application in wearable electronics.

Multiple microstructures

In order to further enhance the sensing performance, there has been increasing interest in engineering multiple microstructures in the flexible pressure sensors. The multiple microstructures include the hierarchy of one microstructure and a combination of different microstructures (Bae et al., 2016; Li et al., 2021b). For example, Zhao et al. reported a hierarchical structure with conical secondary features prepared by exploiting pollen grains of wild chrysanthemum as templates (Figure 7A). The conical secondary features on the hierarchical structure greatly improve the linear relationship between the contact area and applied pressure over a broad range. Thus, the pressure sensor exhibits a high sensitivity of 3.5 kPa^{-1} over an ultrawide sensing range of 0–218 kPa with excellent linearity via a coefficient of 0.997 (Zhao et al., 2020).

Most research on constructing multiple microstructures is in the area of combining diverse microstructures. For example, Yao et al. combined an array of three-dimensional metallic annular cracks and micropyramidal arrays to address the inherent trade-off between sensitivity and hysteresis in tactile sensors when using soft materials (Yao et al., 2020). The sensing mechanism was based upon the synergistic effects of the reconnection of neighboring metal-film segments and the contact area change (Figure 7B). Therefore, the sensors possessed both ultrahigh sensitivity (>10^7 Ω kPa^{-1}) and low hysteresis (2.99 ± 1.37%). Similarly, Yang et al. designed a capacitive pressure sensor based on a dielectric layer with porous micropyramidal structure as shown in Figure 7C (Yang et al., 2019b). The porous pyramidal structure was constructed by the combination of molding micropatterned template and dissolving a sacrificial template. The porous micropyramidal dielectric layer bears the advantages of low compressive modulus and large change in an effective dielectric constant under pressure. As a result, the sensitivity of the sensor drastically improved to 44.5 kPa^{-1} in the pressure range <100 Pa compared to that of the sensor with a solid pyramid dielectric layer. Recently, Zhou et al. synthesized the multiple structure of metal-organic framework (MOF) hybrid array on copper mesh (MHA@Mesh) for a flexible sensor with the template method (Zhou et al., 2020a). The multiple structure was similar to the micro/nanoscale structure of human skin, which provided an efficient interlocking contact (Figure 7D). Therefore, the MHA@Mesh-based pressure sensor exhibits rapid response (<1 ms) and high sensitivity (up to 307 kPa^{-1}), which is 20 times higher than that of MHA@Foil-based sensor (15 kPa^{-1}).

In brief, it can be concluded that engineering microstructures are capable of effectively improving the performance of flexible pressure sensors. But the overall effect of each microstructure may vary from each other. To intuitively reflect the role of each microstructure, the sensitivity variation as a function of sensing range for flexible pressure sensors with different microstructures is summarized in Figure 8. It can be found that constructing micropatterned structures could significantly increase the sensitivity of pressure sensors in the low-pressure regions due to a stress concentration effect. But the sensitivity decreases rapidly with the increase of the applied pressure because the deformation of micropatterns is limited, thus leading to a limited linear sensing range. The pressure sensors with porous microstructures feature a wide sensing range due to their remarkable compressibility, albeit the sensitivity is generally low. The fiber-network microstructures, which also possess hierarchical porous structures constructed by interlacing fibers could endow the sensors with a moderate linear sensing range and higher sensitivity compared with porous microstructures. Engineering multiple microstructures could endow the flexible pressure sensor with both high sensitivity and a wide linear sensing range, benefiting from combining advantages of different microstructures. But the fabrication strategy is relatively complex. Detailed strengths and weaknesses of the flexible pressure sensors with different microstructures are summarized in Table 2.

APPLICATIONS OF FLEXIBLE PRESSURE SENSORS

With the recent advances in performance improvement by engineering microstructures and system-level integration, the applications of flexible pressure sensors have shown broad prospects. One of the promising applications is the wearable human-machine interaction, which allows people to communicate or control machines via tactile sensation (Liu et al., 2020a). Another promising application of flexible pressure sensors is the wearable healthcare monitoring, including *ex vivo* and *in vivo* health monitoring (Li et al., 2020a). Here, we emphatically introduce the major progress of the above three practical applications in the past few years.

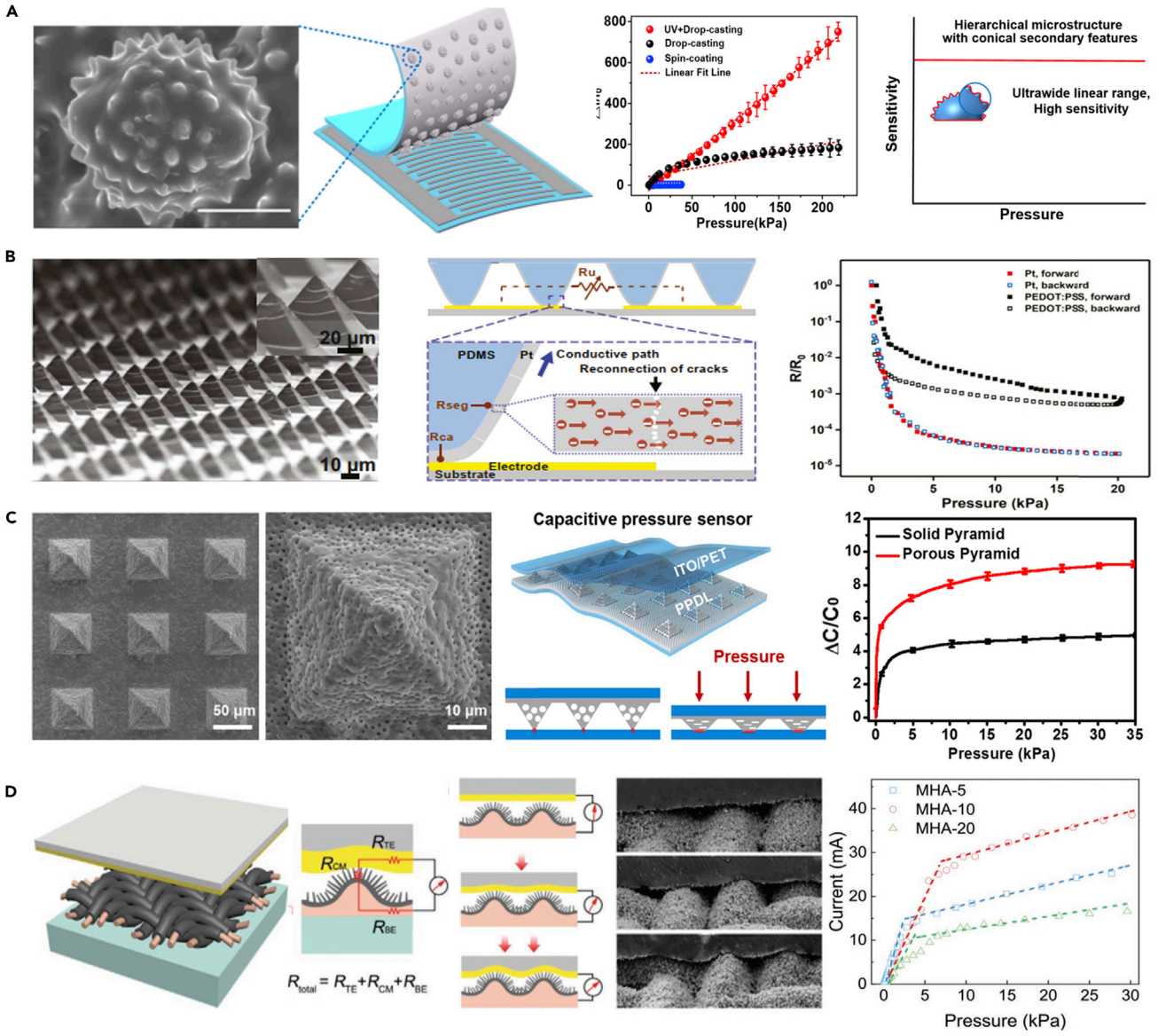

Figure 7. Flexible pressure sensors with multiple microstructures

(A) SEM image of the PDMS film with hierarchical microstructure replicated from the pollen grain, schematic diagram of a piezoresistive sensor composed of the microstructured MWCNT/PDMS film, current response of pressure sensors prepared via spin coating, drop casting, and UV drop casting to pressure, and schematic illustrating the pressure response of the sensor with hierarchical microstructure. Adapted with permission (Zhao et al., 2020). Copyright 2020, American Chemical Society.

(B) SEM image of Pt-coated micropyramidal array with controlled annular cracks, the schematic model of the conductive pathways of the sensor under compressing loads, and the pressure-induced electrical performance of the sensor compared with the PEDOT:PSS-coated micropyramid sensor. Adapted with permission (Yao et al., 2020). Copyright 2020, National Academy of Sciences.

(C) SEM images of dielectric layer with porous pyramid arrays, schematic of capacitive pressure sensor based on the dielectric layer, and relative change in capacitance versus pressure of the sensors. Adapted with permission (Yang et al., 2019b). Copyright 2019, American Chemical Society.

(D) Schematic illustration of the structure of the flexible pressure sensor with hierarchical structure of MOF hybrid array on copper mesh, the proposed pressure sensing mechanism, and pressure-dependent current curves of the sensors with different length of MOF hybrid array under pressure range (0–30 kPa). Adapted with permission (Zhou et al., 2020a). Copyright 2020, Wiley-VCH Verlag GmbH & Co. KGaA, Weinheim.

Applications in wearable human-machine interaction

Our modern lifestyle is increasingly dependent on electronic products, and human-machine interaction plays an important role in improving the user experience today. Wearable human-machine interactions offer the potential of enhancing user experience and revolutionizing user entertainment and are afforded

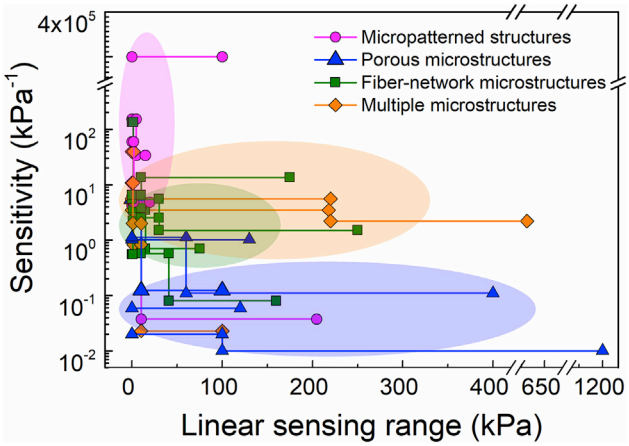

Figure 8. Summary of the sensitivity variation as a function of sensing range for flexible pressure sensors with different microstructures

by the development of flexible pressure sensors that offer appropriate deformability and stretchability (Feng et al., 2021). One of the important applications of flexible pressure sensors in human-machine interaction is intelligent recognition, such as image, voice, gesture, and face recognition (Chen et al., 2022). For example, Syu et al. fabricated a hybrid self-powered sensor by integrating a nanofiber-based piezoelectric sensor and a biomimetic triboelectric sensor with porous PVDF fibers (Syu et al., 2020). The synergistic effect of the hybrid system effectively enhanced the energy harvesting characteristic, which exhibited open-circuit voltage (V_{OC}) of 15 V and 115 nA of short-circuit current and a maximum average power density of 675 $\mu W/m^2$. Furthermore, these sensors were sewed on socks, gloves, and trousers to distinguish five different human motions (i.e., elbow bending up to 45°, elbow bending up to 90°, clapping, leg lifting, and stepping) by recording the average V_{OC} signals. This gesture recognition can be realized by introducing the machine learning algorithm of long short-term memory, showing an overall training accuracy of 82.3% (Figure 9A).

In addition, interactive control is another important application of human-machine interaction. The human-machine interface is the communication bridge between humans and machines, and involves obtaining input signals from users and converting to instructions to allow the machine to perform specific actions (Zhao et al., 2021a). A wearable human-machine interaction system based on flexible pressure sensors can significantly improve the interactive accuracy and user experience of the control process. For example, Zhong et al. fabricated a high-performance piezoresistive pressure sensor with wide linear range and high sensitivity by employing a micronano hybrid conductive elastomer film with arched micropatterned structure (Zhong et al., 2021). Then, the sensors were affixed to a textile glove at knuckle regions, establishing a human-machine interface as shown in Figure 9B. The smart glove system could record and process the bending signals from each joint to control the robot hand in real time, such as gesture imitation and grabbing objects. Wang et al. designed a stretchable textile-based single-electrode TENG consisting of the porous flexible layer and waterproof flexible conductive fabric (Wang et al., 2021b). The resultant TENG exhibited high outputs (~135 V, ~7.5 μA, 26 $\mu C/m^2$, 631.5 mW/m^2) attributable to the 3D porous microstructure. Integrating the TENG with microelectronic modules, a portable and wearable self-powered haptic controller was fabricated for human-machine interaction as shown in Figure 9C. Specifically, two haptic controllers were simultaneously placed on a commercial arm guard sleeve to act as wearable intelligent controllers, conveniently controlling the operation of lamps, electronic badges, slides, and humidifiers, among other devices.

Applications in *ex vivo* health monitoring

The physiological activities of the human body, such as breath, heartbeat, pulse, and joint movements generate unique pressure signals with different amplitude. Detecting those pressure signals using flexible pressure sensors can enable the continuous monitoring of physiological signals, critical for *ex vivo* healthcare applications for early detection and diagnosis (Wu et al., 2020a). Flexible pressure sensors that are attached to different parts of the body can capture different physiological signals. Yang et al. designed

Table 2. Strengths and weaknesses of the flexible pressure sensors with different microstructures

Microstructure types	Strengths	Weaknesses
Micropatterned structure	Very high sensitivity in low-pressure area Fast response High uniformity	Limited linear sensing range Poor scalability
Porous microstructure	Wide linear sensing range Easy fabrication	Low sensitivity High hysteresis Slow response Poor uniformity
Fiber-network microstructure	High sensitivity Moderate linear sensing range Breathability	Poor uniformity Poor tunability
Multiple microstructure	High sensitivity Wide linear sensing range Fast response	Poor scalability Poor uniformity Poor tunability

a flexible piezoresistive pressure sensor by sandwiching a hierarchical nanofiber film between two interlocking microdome-structured electrodes (Yang et al., 2021b). Benefiting from the hierarchical microstructure, the sensor exhibited an ultrahigh sensitivity of 53 kPa^{-1}, a pressure sensing range from 58.4 to 960 Pa, a fast response time of 38 ms, and good working stability over 50,000 cycles. Moreover, the sensor can be conformally adhered to skin applied in *ex vivo* health monitoring, as shown in Figure 10A. For example, by attaching the sensor to the wrist, the heart rate of 67 beats per minute can be calculated from the radial pulse signals detected by the sensor. Moreover, the sensor could accurately record the deformation of the index finger. The enlargement of bending angles of the index finger will lead to changes in current amplitudes, which can be utilized to access activities in rehabilitation.

In addition, gait analysis, as with blood pressure and body temperature, can reflect the health status and pathological features of the human body from different angles. Real-time gait monitoring is widely used in various healthcare applications, such as dynamic monitoring of Parkinson disease, and early diagnosis and rehabilitation assessment of pes planus (Lu et al., 2021; Tang et al., 2019). Gait monitoring can be realized by integrating flexible pressure sensors into a sensor array to measure the plantar pressure distribution. In this area, Wu et al. designed a low-cost flexible pressure sensor with positive resistance-pressure response based on laser scribing graphene with a multilayer structure (Wu et al., 2020a). This sensor was modulated to achieve both high sensitivity and broad sensing range, useful in detecting plantar pressure. As shown in Figure 10B, several sensors were attached to an insole and integrated with electronic modules to assemble a wearable gait monitoring system that wirelessly provided real-time gait analysis.

More importantly, flexible pressure sensors can be used to monitor cardiovascular diseases that account for the highest mortality globally (Petritz et al., 2021; Song et al., 2018). Chen et al. reported a TENG-based pressure sensor with hierarchical elastomer microstructures to achieve high sensitivity (7.989 V/kPa), wide working pressure range (0.1–60 kPa), fast response (40 ms), high signal-to-noise ratio (38 db), and high stability (Chen et al., 2020c). This comprehensive, excellent sensing performance enabled the sensor to successfully capture arterial pulse wave and distinguish the three characteristic peaks of the pulse wave. The carotid and radial pulse waves were simultaneously recorded to extract the pulse transit time that is defined as the time traveling from carotid artery to radial artery (Figure 10C). Finally, the continuous blood pressure was able to be estimated based on the pulse transit time according to the Moens-Korteweg's formula. Thus, a continuous, non-invasive, and cuff-less blood pressure monitoring approach was realized, which is potentially crucial for early diagnosis and prevention of cardiovascular diseases (Xu et al., 2021).

Applications in *in vivo* health monitoring

Besides the *ex vivo* pressure signals generated by the physiological activities, a variety of internal pressures such as ureteral peristalsis pulse, gastric peristalsis, intracranial pressure, and intraocular pressure can also be detected by implanted flexible pressure sensors (Li et al., 2020a). For example, Zhao et al. designed a piezoresistive pressure sensor by employing PVA as a crosslinker to connect the MXene sheets into a layered network

Figure 9. Applications of flexible pressure sensors in wearable human-machine interaction

(A) Application of a flexible self-powered pressure sensor in gesture recognition through machine learning algorithm. Adapted with permission (Syu et al., 2020). Copyright 2020, Elsevier Ltd.

(B) Application of the pressure sensor in real-time controlling of robot hand. Adapted with permission (Zhong et al., 2021). Copyright 2021, Elsevier Ltd.

(C) Application of the TENG-based pressure sensor in wearable haptic controllers such as controlling light switch states, electronic badges, slides, and humidifiers. Adapted with permission (Wang et al., 2021b). Copyright 2021, Elsevier Ltd.

structure through strong hydrogen bonding (Zhao et al., 2021b). The sensor shows stable performance that can last for over half a year in harsh environments, including aqueous, strong acidic, and alkaline environments. Moreover, the *in vitro* and *in vivo* tests demonstrate that the pressure sensor has good biocompatibility, which is imperative for *in vivo* biomedical applications. Thus, the sensor could be implanted into a *BALB/c* mouse and tested *in vivo*. Specifically, the sensor was first attached to the epicardial tip of the heart to obtain a strong electrocardiograph (ECG) signal with high sensitivity and SD (Figure 11A). Then, the gastric peristalsis could be detected by placing the sensor on the serous membrane of the outermost gastric wall.

In addition, iatrogenic ureteral injury is a common problem during surgery, especially in gynecologic, colorectal, and pelvic surgeries. Identification of the ureter is difficult by visual inspection due to its

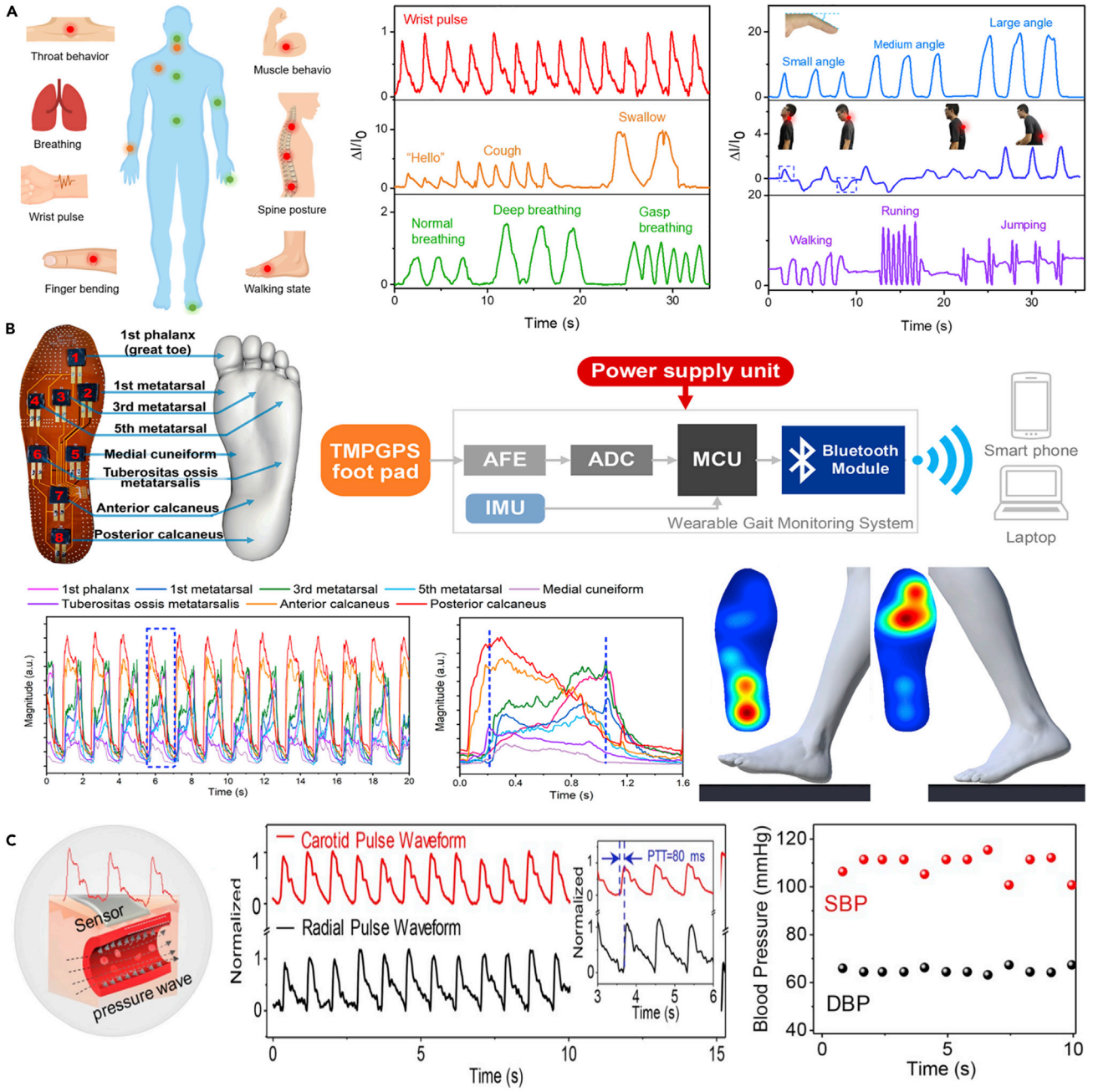

Figure 10. Applications of flexible pressure sensors in *ex vivo* health monitoring

(A) Application of flexible pressure sensor in monitoring human physiological signals and motion signals. Adapted with permission (Yang et al., 2021b). Copyright 2021, American Chemical Society.

(B) Application of flexible pressure sensor in plantar pressure detection and gait monitoring. Adapted with permission (Wu et al., 2020a). Copyright 2020, American Chemical Society.

(C) Application of the TENG-based pressure sensor in pulse wave detection and continuous blood pressure monitoring. Adapted with permission (Chen et al., 2020c). Copyright 2020, Elsevier Ltd.

inconspicuous anatomical location. To address this problem, Wang et al. proposed high-performance tubular porous pressure sensors to identify the ureter *in situ* intraoperatively (Wang et al., 2021d). The porous pressure sensors were fabricated by using uniform silicon dioxide microspheres as sacrificial templates that could be dissolved by hydrofluoric acid, leaving uniform pores. The uniform porous structure

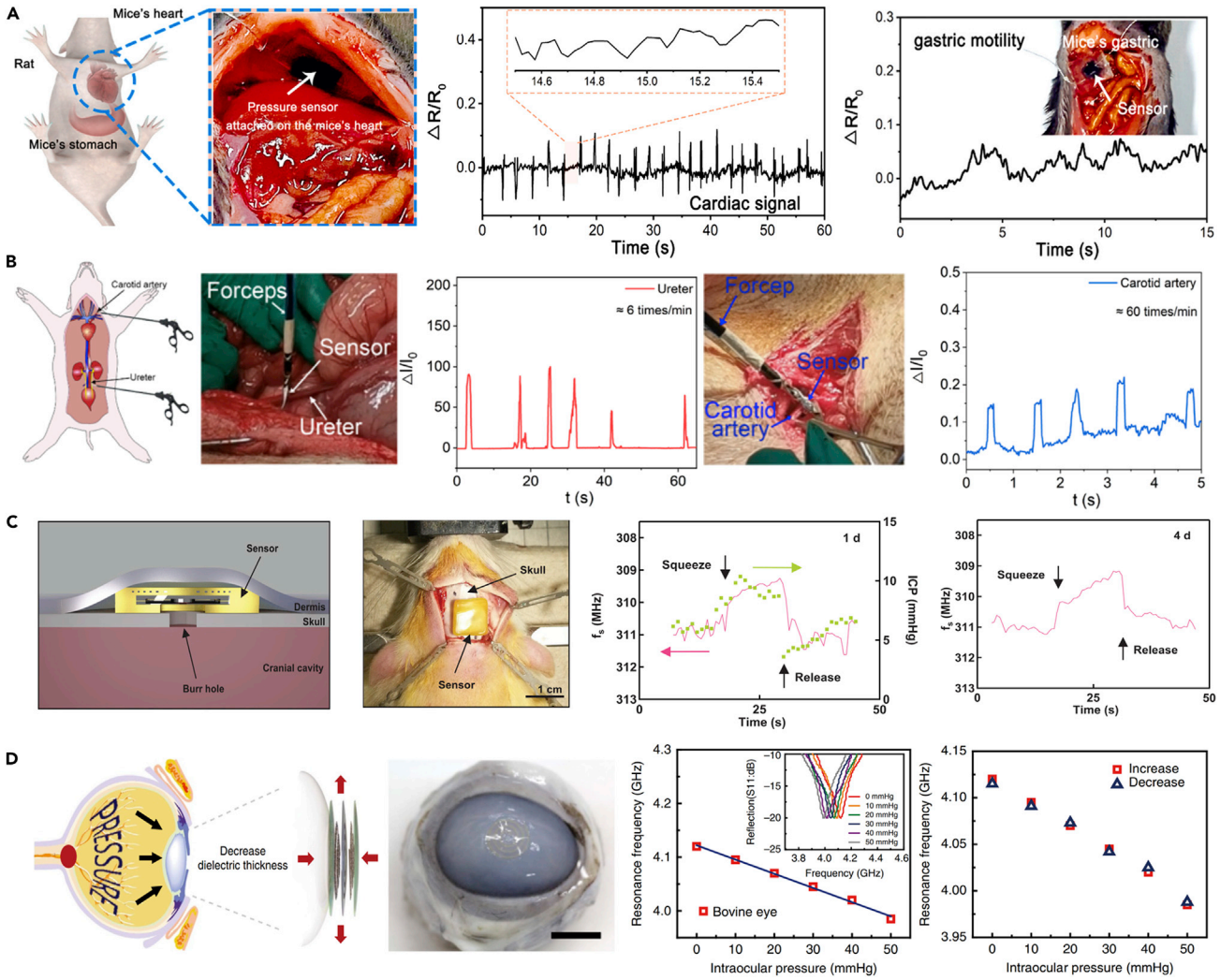

Figure 11. Applications of flexible pressure sensors in *in vivo* health monitoring

(A) Application of flexible pressure sensor in study heart and gastric dynamics of mice. Adapted with permission (Zhao et al., 2021b). Copyright 2021, Elsevier Ltd.

(B) Application of flexible piezoresistive pressure sensor in *in situ* monitoring the carotid artery and ureter of a female Bama minipig. Adapted with permission (Wang et al., 2021d). Copyright 2021, American Chemical Society.

(C) Application of the bioresorbable wireless pressure sensor in measuring intracranial pressure of rats. Adapted with permission (Lu et al., 2020). Copyright 2020, Wiley-VCH GmbH.

(D) Application of the wearable pressure sensor in monitoring intraocular pressure of bovine eye. Adapted with permission (Kim et al., 2017). Copyright 2017, Nature Publishing Group.

contributed to a high sensitivity of 448.2 kPa^{-1}, high reproducibility, and low sensor-to-sensor variation of 3.29%. Incorporating the sensors with forceps can monitor the ureteral peristalsis pulses (6 times/min) and carotid artery pulses (60 times/min) of a female Bama minipig *in situ* intraoperatively (Figure 11B). Thus, the ureter could be recognized in real time by monitoring the frequency of pressure pulses.

More importantly, accurate measurement of *in vivo* pressures can provide essential diagnostic information for many life-threatening medical conditions. For example, intracranial pressure (ICP) is a key monitor parameter for the patients after traumatic brain injury, the increasing of which can impede blood flow and lead to ischemia (Yang et al., 2021a). Recently, Lu et al. reported a bioresorbable, wireless pressure sensor based on passive inductor-capacitor resonance circuits in layouts with optimal sensitivity of 200 kHz/mmHg and resolution of 1 mmHg (Lu et al., 2020). The measurement of ICP for a rat model was conducted by attaching the sensor over a burr hole drilled through the skull, connecting the cranial cavity to the

sensor (Figure 11C). This sensor could capture changes in ICP after squeezing the flank of the rat and the *in vivo* measurement was held stable for up to 96 h (four days). Furthermore, this sensor gradually dissolves completely in biofluids because all the constituent materials are bioresorbable, thus avoiding any extraction surgeries. Another significant health indicator in *in vivo* health monitoring is intraocular pressure (IOP). It is known that the increasing IOP triggered by glaucoma can lead to blindness. Therefore, accurate and continuous IOP monitoring is important for the early diagnosis and treatment of glaucoma. Kim et al. developed a transparent contact lens sensor by placing two inductive spirals made of graphene-AgNW hybrid electrodes on both sides of a silicone elastomer film (Kim et al., 2017). These sensors can simultaneously monitor glucose within tears and IOP by analyzing the change in electrical signals. Specifically, high IOP will increase the corneal radius of curvature, which in turn improves both the inductance by biaxial lateral expansion of the spiral coils and the capacitance by thinning the dielectric. In this way, the elevated IOP will decrease the resonance frequency of the sensor. The sensor was then transferred onto the contact lens worn by a bovine eyeball *in vitro* (Figure 11D). The frequency response of this sensor was nearly linear for relatively small pressure and showed good reproducibility with negligible hysteresis.

CONCLUSION AND OUTLOOKS

Flexible pressure sensors, as the key devices for obtaining external force information, are core components of flexible electronics, which play essential roles in many fields, such as wearable human-machine interaction and healthcare monitoring. There is an increasing demand for pressure sensors with high performances, such as high sensitivity, broad linear sensing range, fast response, low hysteresis, and good durability. Engineering microstructures in the pressure sensor are a rapidly emerging and efficient method to meet these often-contrasting performance requirements. In this review, we highlighted high-performance flexible pressure sensors via engineering different microstructure architectures implemented in recent years, including micropatterned, porous, fiber-network, and multiple microstructures. The effect of microstructures on pressure sensing performance was discussed to provide researchers with a better understanding of their implementation mechanism, and to guide them in the future exploration and design of pressure sensors with novel microstructures aimed toward overall high performance. Ultimately, we highlight the applications of high-performance flexible pressure sensors with microstructures in wearable human-machine interaction, and in *ex vivo* and *in vivo* health monitoring.

Even though achieving high-performance flexible pressure sensors via engineering microstructures have been widely studied and considerable advances have been made in academia, there is still a long way forward for flexible pressure sensors to penetrate real-world practical applications. The challenges of limiting their applications and the corresponding recommended solutions are as follows.

Firstly, the large-area preparation of microstructures with controllable morphology, size, and distribution remains a significant challenge. It has been shown that the silicon template method can offer controllable morphology, size, and distribution, but it cannot realize large-area fabrication because of the high cost and complex process. Although employing the natural materials or commercially available materials as the template address the aforementioned challenge, and can offer low cost and simple process, its structural design is not controllable. Therefore, it is crucial to develop advanced preparation methods, such as 3D printing, microelectronic printing, and laser processing, to fabricate controllable microstructures with large area and low cost.

Secondly, working stability is a key parameter for pressure sensors in practical applications. The current measurement of the working stability for pressure sensors is mainly conducted under repeated loading-unloading in normal environmental conditions. However, in real applications, the sensor will encounter complex and harsh environment conditions, such as high humidity, perspiration, and even erosion of bodily fluids when implanted, which may influence the stability of microstructures and the performance of sensors in long-term use consequently. Thus, the mechanisms of working stability in simulated harsh environments should be further investigated. Moreover, effective packing technologies with minimal influence on the microstructure and sensing performance should be explored in developing pressure sensors toward practical applications.

Thirdly, because the pressure sensors applied in wearable human-machine interaction and healthcare monitoring are placed directly onto the human skin or implanted into the body, it raises concerns for the safety and comfort for humans during use. Thus, a variety of materials, including substrate materials,

active materials, and electrode materials with good biocompatibility should be further developed. Moreover, for the *in vivo* health monitoring applications, utilizing implantable sensors comprising bioresorbable or biodegradable materials can avoid surgical removal and reduce the risk of infection. Thus, the need to develop biocompatible and biodegradable materials for pressure sensors in human-related applications is imperative.

Fourthly, it is noted that pressure sensor can work only when it is integrated into the pressure sensing system with other components, including a wireless transmission unit, a signal transduction unit, information processing, memory, a feedback unit, and power sources. The realization of the flexible pressure sensing system depends on the comprehensive development of flexible electronics, which calls for multidisciplinary efforts.

Despite such challenges, the development of high-performance flexible pressure sensors via engineering microstructures is rapidly gaining significant attention. The advent of new materials, microstructures, and advanced fabrication strategies will greatly support in advancing flexible pressure sensors with excellent comprehensive performance. The improved performance of flexible pressure sensors can further enable novel applications in broader fields. Combined with the emergence and development of new technologies and concepts, such as Metaverse and Internet of Things, flexible pressure sensors have broad application prospect in future digital and intelligent technologies for monitoring real-time physiological signals, providing tactile feedback, and improving user experience.

ACKNOWLEDGMENTS

This work was financially supported by Zhejiang Provincial Natural Science Foundation of China (LQ22E030005), the National Natural Science Foundation of China (52103081), the Australian Research Council (Nos. DP190102992 and FT190100188), Science and Technology Program of Jiaxing City (2020AD10012), and the Top-level Talent Project of Zhejiang Province.

AUTHOR CONTRIBUTIONS

Conceptualization, X.C. and Z.X.; investigation, X.C., F.H., X.Z., H.Z., P.S., and H.W.; writing-original draft, X.C.; writing-review & editing, H.Z., V.C., P.S., H.W., and Z.X.; funding acquisition, X.C. and Z.X. All authors read and discussed the manuscript.

DECLARATION OF INTERESTS

The authors declare no competing interests.

REFERENCES

Amit, M., Chukoskie, L., Skalsky, A.J., Garudadri, H., and Ng, T.N. (2020). Flexible pressure sensors for objective assessment of motor disorders. Adv. Funct. Mater. *30*, 1905241.

Bae, G.Y., Pak, S.W., Kim, D., Lee, G., Kim Do, H., Chung, Y., and Cho, K. (2016). Linearly and highly pressure-sensitive electronic skin based on a bioinspired hierarchical structural array. Adv. Mater. *28*, 5300–5306.

Bai, N., Wang, L., Wang, Q., Deng, J., Wang, Y., Lu, P., Huang, J., Li, G., Zhang, Y., Yang, J., et al. (2020). Graded intrafillable architecture-based iontronic pressure sensor with ultra-broad-range high sensitivity. Nat. Commun. *11*, 209.

Bi, L.L., Yang, Z.L., Chen, L.J., Wu, Z., and Ye, C. (2020). Compressible AgNWs/$Ti_3C_2T_x$ MXene aerogel-based highly sensitive piezoresistive pressure sensor as versatile electronic skins. J. Mater. Chem. A *8*, 20030–20036.

Cai, L., Chen, G.X., Tian, J.F., Su, B., and He, M.H. (2021). Three-dimensional printed ultrahighly sensitive bioinspired ionic skin based on submicrometer-scale structures by polymerization shrinkage. Chem. Mater. *33*, 2072–2079.

Chao, M., He, L., Gong, M., Li, N., Li, X., Peng, L., Shi, F., Zhang, L., and Wan, P. (2021). Breathable $Ti_3C_2T_x$ MXene/protein nanocomposites for ultrasensitive medical pressure sensor with degradability in solvents. ACS Nano *15*, 9746–9758.

Chen, M., Xia, J., Zhou, J., Zeng, Q., Li, K., Fujisawa, K., Fu, W., Zhang, T., Zhang, J., Wang, Z., et al. (2017). Ordered and atomically perfect fragmentation of layered transition metal dichalcogenides via mechanical instabilities. ACS Nano *11*, 9191–9199.

Chen, J., Yu, Q., Cui, X., Dong, M., Zhang, J., Wang, C., Fan, J., Zhu, Y., and Guo, Z. (2019a). An overview of stretchable strain sensors from conductive polymer nanocomposites. J. Mater. Chem. C *7*, 11710–11730.

Chen, M., Li, K., Cheng, G., He, K., Li, W., Zhang, D., Li, W., Feng, Y., Wei, L., Li, W., et al. (2019b). Touchpoint-tailored ultrasensitive piezoresistive pressure sensors with a broad dynamic response range and low detection limit. ACS Appl. Mater. Interfaces *11*, 2551–2558.

Chen, J., Zhu, Y., and Jiang, W. (2020a). A stretchable and transparent strain sensor based on sandwich-like PDMS/CNTs/PDMS composite containing an ultrathin conductive CNT layer. Compos. Sci. Technol. *186*, 107938.

Chen, M., Wang, Z., Ge, X., Wang, Z., Fujisawa, K., Xia, J., Zeng, Q., Li, K., Zhang, T., Zhang, Q., et al. (2020b). Controlled fragmentation of single-atom-thick polycrystalline graphene. Matter *2*, 666–679.

Chen, S., Wu, N., Lin, S., Duan, J., Xu, Z., Pan, Y., Zhang, H., Xu, Z., Huang, L., Hu, B., and Zhou, J. (2020c). Hierarchical elastomer tuned self-powered pressure sensor for wearable multifunctional cardiovascular electronics. Nano Energy *70*, 104460.

Chen, X., Shao, J., Tian, H., Li, X., Wang, C., Luo, Y., and Li, S. (2020d). Scalable imprinting of flexible multiplexed sensor arrays with distributed piezoelectricity-enhanced micropillars for

dynamic tactile sensing. Adv. Mater. Technol. *5*, 2000046.

Chen, J., Zhang, J., Hu, J., Luo, N., Sun, F., Venkatesan, H., Zhao, N., and Zhang, Y. (2021a). Ultrafast-response/recovery flexible piezoresistive sensors with DNA-like double helix yarns for epidermal pulse monitoring. Adv. Mater. e2104313.

Chen, J.W., Zhu, Y.T., Chang, X.H., Pan, D., Song, G., Guo, Z.H., and Naik, N. (2021b). Recent progress in essential functions of soft electronic skin. Adv. Funct. Mater. *31*, 2104686.

Chen, J.W., Zhu, Y.T., Huang, J.R., Zhang, J.X., Pan, D., Zhou, J.Y., Ryu, J.E., Umar, A., and Guo, Z.H. (2021c). Advances in responsively conductive polymer composites and sensing applications. Polym. Rev. *61*, 157–193.

Chen, S., Li, J., Liu, H., Shi, W., Peng, Z., and Liu, L. (2022). Pruney fingers-inspired highly stretchable and sensitive piezoresistive fibers with isotropic wrinkles and robust interfaces. Chem. Eng. J. *430*, 133005.

Cheng, Y., Ma, Y., Li, L., Zhu, M., Yue, Y., Liu, W., Wang, L., Jia, S., Li, C., Qi, T., et al. (2020). Bioinspired microspines for a high-performance spray $Ti_3C_2T_x$ MXene-based piezoresistive sensor. ACS Nano *14*, 2145–2155.

Choong, C.L., Shim, M.B., Lee, B.S., Jeon, S., Ko, D.S., Kang, T.H., Bae, J., Lee, S.H., Byun, K.E., Im, J., et al. (2014). Highly stretchable resistive pressure sensors using a conductive elastomeric composite on a micropyramid array. Adv. Mater. *26*, 3451–3458.

Cui, X., Jiang, Y., Xu, Z., Xi, M., Jiang, Y., Song, P., Zhao, Y., and Wang, H. (2021). Stretchable strain sensors with dentate groove structure for enhanced sensing recoverability. Compos. Part B *211*, 108641.

Cui, X., Chen, J., Wu, W., Liu, Y., Li, H., Xu, Z., and Zhu, Y. (2022). Flexible and breathable all-nanofiber iontronic pressure sensors with ultraviolet shielding and antibacterial performances for wearable electronics. Nano Energy *95*, 107022.

Dai, S.-W., Gu, Y.-L., Zhao, L., Zhang, W., Gao, C.-H., Wu, Y.-X., Shen, S.-C., Zhang, C., Kong, T.-T., Li, Y.-T., et al. (2021). Bamboo-inspired mechanically flexible and electrically conductive polydimethylsiloxane foam materials with designed hierarchical pore structures for ultra-sensitive and reliable piezoresistive pressure sensor. Compos. Part B *225*, 109243.

Ding, Y., Xu, T., Onyilagha, O., Fong, H., and Zhu, Z. (2019). Recent advances in flexible and wearable pressure sensors based on piezoresistive 3D monolithic conductive sponges. ACS Appl. Mater. Interfaces *11*, 6685–6704.

Du, Q., Liu, L., Tang, R., Ai, J., Wang, Z., Fu, Q., Li, C., Chen, Y., and Feng, X. (2021). High-performance flexible pressure sensor based on controllable hierarchical microstructures by laser scribing for wearable electronics. Adv. Mater. Technol. *6*, 2100122.

Feng, B., Jiang, X., Zou, G.S., Wang, W.G., Sun, T.M., Yang, H., Zhao, G.L., Dong, M.Y., Xiao, Y., Zhu, H.W., and Liu, L. (2021). Nacre-inspired, liquid metal-based ultrasensitive electronic skin by spatially regulated cracking strategy. Adv. Funct. Mater. *31*, 2102359.

Fu, M., Zhang, J., Jin, Y., Zhao, Y., Huang, S., and Guo, C.F. (2020). A highly sensitive, reliable, and high-temperature-resistant flexible pressure sensor based on ceramic nanofibers. Adv. Sci. *7*, 2000258.

Fu, X.Y., Wang, L.L., Zhao, L.J., Yuan, Z.Y., Zhang, Y.P., Wang, D.Y., Wang, D.P., Li, J.Z., Li, D.D., Shulga, V., et al. (2021). Controlled assembly of mxene nanosheets as an electrode and active layer for high-performance electronic skin. Adv. Funct. Mater. *31*, 2010533.

Gao, Y., Yu, L., Yeo, J.C., and Lim, C.T. (2019). Flexible hybrid sensors for health monitoring: materials and mechanisms to render wearability. Adv. Mater. *32*, 1902133.

Gong, M., Zhang, L., and Wan, P. (2020). Polymer nanocomposite meshes for flexible electronic devices. Prog. Poly. Sci. *107*, 101279.

Guan, X., Wang, Z., Zhao, W., Huang, H., Wang, S., Zhang, Q., Zhong, D., Lin, W., Ding, N., and Peng, Z. (2020). Flexible piezoresistive sensors with wide-range pressure measurements based on a graded nest-like architecture. ACS Appl. Mater. Interfaces *12*, 26137–26144.

Guo, W., Tan, C., Shi, K., Li, J., Wang, X.X., Sun, B., Huang, X., Long, Y.Z., and Jiang, P. (2018). Wireless piezoelectric devices based on electrospun PVDF/$BaTiO_3$ NW nanocomposite fibers for human motion monitoring. Nanoscale *10*, 17751–17760.

Guo, Y., Zhong, M., Fang, Z., Wan, P., and Yu, G. (2019). A wearable transient pressure sensor made with MXene nanosheets for sensitive broad-range human-machine interfacing. Nano Lett. *19*, 1143–1150.

Han, Z., Cheng, Z., Chen, Y., Li, B., Liang, Z., Li, H., Ma, Y., and Feng, X. (2019a). Fabrication of highly pressure-sensitive, hydrophobic, and flexible 3D carbon nanofiber networks by electrospinning for human physiological signal monitoring. Nanoscale *11*, 5942–5950.

Han, Z., Li, H., Xiao, J., Song, H., Li, B., Cai, S., Chen, Y., Ma, Y., and Feng, X. (2019b). Ultralow-cost, highly sensitive, and flexible pressure sensors based on carbon black and airlaid paper for wearable electronics. ACS Appl. Mater. Interfaces *11*, 33370–33379.

He, J., Zhang, Y., Zhou, R., Meng, L., Chen, T., Mai, W., and Pan, C. (2020a). Recent advances of wearable and flexible piezoresistivity pressure sensor devices and its future prospects. J. Materiomics *6*, 86–101.

He, K., Hou, Y., Yi, C., Li, N., Sui, F., Yang, B., Gu, G., Li, W., Wang, Z., Li, Y., et al. (2020b). High-performance zero-standby-power-consumption-under-bending pressure sensors for artificial reflex arc. Nano Energy *73*, 104743.

He, F.L., You, X.Y., Wang, W.G., Bai, T., Xue, G.F., and Ye, M.D. (2021). Recent progress in flexible microstructural pressure sensors toward human-machine interaction and healthcare applications. Small Methods *5*, 2001041.

Jang, G.N., Hong, S.Y., Park, H., Lee, Y.H., Park, H., Lee, H., Jeong, Y.R., Jin, S.W., Keum, K., and Ha, J.S. (2021). Highly sensitive pressure and temperature sensors fabricated with poly(3-hexylthiophene-2,5-diyl)-coated elastic carbon foam for bio-signal monitoring. Chem. Eng. J. *423*, 130197.

Ji, B., Mao, Y., Zhou, Q., Zhou, J., Chen, G., Gao, Y., Tian, Y., Wen, W., and Zhou, B. (2019). Facile preparation of hybrid structure based on mesodome and micropillar arrays as flexible electronic skin with tunable sensitivity and detection range. ACS Appl. Mater. Interfaces *11*, 28060–28071.

Jung, Y., Lee, T., Oh, J., Park, B.-G., Ko, J.S., Kim, H., Yun, J.P., and Cho, H. (2021). Linearly sensitive pressure sensor based on a porous multistacked composite structure with controlled mechanical and electrical properties. ACS Appl. Mater. Interfaces *13*, 28975–28984.

Kim, J., Kim, M., Lee, M.S., Kim, K., Ji, S., Kim, Y.T., Park, J., Na, K., Bae, K.H., Kyun Kim, H., et al. (2017). Wearable smart sensor systems integrated on soft contact lenses for wireless ocular diagnostics. Nat. Commun. *8*, 14997.

Kim, S., Amjadi, M., Lee, T.-I., Jeong, Y., Kwon, D., Kim, M.S., Kim, K., Kim, T.-S., Oh, Y.S., and Park, I. (2019). Wearable, ultrawide-range, and bending-insensitive pressure sensor based on carbon nanotube network-coated porous elastomer sponges for human interface and healthcare devices. ACS Appl. Mater. Interfaces *11*, 23639–23648.

Kong, H.J., Song, Z.Q., Xu, J.N., Qu, D.Y., Bao, Y., Wang, W., Wang, Z.X., Zhang, Y.W., Ma, Y.M., Han, D.X., and Niu, L. (2020). Untraditional deformation-driven pressure sensor with high sensitivity and ultra-large sensing range up to MPa enables versatile applications. Adv. Mater. Technol. *5*, 2000677.

Lee, Y., Park, J., Cho, S., Shin, Y.E., Lee, H., Kim, J., Myoung, J., Cho, S., Kang, S., Baig, C., and Ko, H. (2018). Flexible ferroelectric sensors with ultrahigh pressure sensitivity and linear response over exceptionally broad pressure range. ACS Nano *12*, 4045–4054.

Lee, S., Franklin, S., Hassani, F.A., Yokota, T., Nayeem, M.O.G., Wang, Y., Leib, R., Cheng, G., Franklin, D.W., and Someya, T. (2020). Nanomesh pressure sensor for monitoring finger manipulation without sensory interference. Science *370*, 966–970.

Lee, J., Ihle, S.J., Pellegrino, G.S., Kim, H., Yea, J., Jeon, C.Y., Son, H.C., Jin, C., Eberli, D., Schmid, F., et al. (2021a). Stretchable and suturable fibre sensors for wireless monitoring of connective tissue strain. Nat. Electron. *4*, 291–301.

Lee, Y., Myoung, J., Cho, S., Park, J., Kim, J., Lee, H., Lee, Y., Lee, S., Baig, C., and Ko, H. (2021b). Bioinspired gradient conductivity and stiffness for ultrasensitive electronic skins. ACS Nano *15*, 1795–1804.

Lee, Y., and Ahn, J.H. (2020). Biomimetic tactile sensors based on nanomaterials. ACS Nano *14*, 1220–1226.

Li, W., He, K., Zhang, D., Li, N., Hou, Y., Cheng, G., Li, W., Sui, F., Dai, Y., Luo, H., et al. (2019). Flexible and high performance piezoresistive pressure

sensors based on hierarchical flower-shaped $SnSe_2$ nanoplates. ACS Appl. Energ. Mater. *2*, 2803–2809.

Li, L., Zheng, J., Chen, J., Luo, Z., Su, Y., Tang, W., Gao, X., Li, Y., Cao, C., Liu, Q., et al. (2020a). Flexible pressure sensors for biomedical applications: from ex vivo to in vivo. Adv. Mater. Interfaces *7*, 2000743.

Li, X., Fan, Y.J., Li, H.Y., Cao, J.W., Xiao, Y.C., Wang, Y., Liang, F., Wang, H.L., Jiang, Y., Wang, Z.L., and Zhu, G. (2020b). Ultracomfortable hierarchical nanonetwork for highly sensitive pressure sensor. ACS Nano *14*, 9605–9612.

Li, H., Ma, Y., and Huang, Y. (2021a). Material innovation and mechanics design for substrates and encapsulation of flexible electronics: a review. Mater. Horiz. *8*, 383–400.

Li, W., Jin, X., Han, X., Li, Y.R., Wang, W.Y., Lin, T., and Zhu, Z.T. (2021b). Synergy of porous structure and microstructure in piezoresistive material for high-performance and flexible pressure sensors. ACS Appl. Mater. Interfaces *13*, 19211–19220.

Lin, Q., Huang, J., Yang, J., Huang, Y., Zhang, Y., Wang, Y., Zhang, J., Wang, Y., Yuan, L., Cai, M., et al. (2020). Highly sensitive flexible iontronic pressure sensor for fingertip pulse monitoring. Adv. Healthc. Mater. *9*, 2001023.

Liu, X., Su, G., Guo, Q., Lu, C., Zhou, T., Zhou, C., and Zhang, X. (2018). Hierarchically structured self-healing sensors with tunable positive/negative piezoresistivity. Adv. Funct. Mater. *28*, 1706658.

Liu, R., Li, J., Li, M., Zhang, Q., Shi, G., Li, Y., Hou, C., and Wang, H. (2020a). MXene-coated air-permeable pressure-sensing fabric for smart wear. ACS Appl. Mater. Interfaces *12*, 46446–46454.

Liu, S., Wang, S., Xuan, S., Zhang, S., Fan, X., Jiang, H., Song, P., and Gong, X. (2020b). Highly flexible multilayered e-skins for thermal-magnetic-mechanical triple sensors and intelligent grippers. ACS Appl. Mater. Interfaces *12*, 15675–15685.

Liu, H., Chen, X.Y., Zheng, Y.J., Zhang, D.B., Zhao, Y., Wang, C.F., Pan, C.F., Liu, C.T., and Shen, C.Y. (2021). Lightweight, superelastic, and hydrophobic polyimide nanofiber/MXene composite aerogel for wearable piezoresistive sensor and oil/water separation applications. Adv. Funct. Mater. *31*, 2008006.

Lu, D., Yan, Y., Deng, Y., Yang, Q., Zhao, J., Seo, M.H., Bai, W., MacEwan, M.R., Huang, Y., Ray, W.Z., and Rogers, J.A. (2020). Bioresorbable wireless sensors as temporary implants for in vivo measurements of pressure. Adv. Funct. Mater. *30*, 2003754.

Lu, P., Wang, L., Zhu, P., Huang, J., Wang, Y.J., Bai, N.N., Wang, Y., Li, G., Yang, J.L., Xie, K.W., et al. (2021). Iontronic pressure sensor with high sensitivity and linear response over a wide pressure range based on soft micropillared electrodes. Sci. Bull. *66*, 1091–1100.

Luo, J., Gao, W., and Wang, Z.L. (2021). The triboelectric nanogenerator as an innovative technology toward intelligent sports. Adv. Mater. *33*, e2004178.

Ma, C., Xu, D., Huang, Y.-C., Wang, P., Huang, J., Zhou, J., Liu, W., Li, S.-T., Huang, Y., and Duan, X. (2020). Robust flexible pressure sensors made from conductive micropyramids for manipulation tasks. ACS Nano *14*, 12866–12876.

Min, P., Li, X.F., Liu, P.F., Liu, J., Jia, X.Q., Li, X.P., and Yu, Z.Z. (2021). Rational design of soft yet elastic lamellar graphene aerogels via bidirectional freezing for ultrasensitive pressure and bending sensors. Adv. Funct. Mater. *31*, 2103703.

Niu, H., Zhang, H., Yue, W., Gao, S., Kan, H., Zhang, C., Zhang, C., Pang, J., Lou, Z., Wang, L., et al. (2021). Micro-nano processing of active layers in flexible tactile sensors via template methods: a review. Small *17*, e2100804.

Pan, H., and Lee, T.W. (2021). Recent progress in development of wearable pressure sensors derived from biological materials. Adv. Healthc. Mater. *10*, e2100460.

Peng, S., Blanloeuil, P., Wu, S., and Wang, C.H. (2018). Rational design of ultrasensitive pressure sensors by tailoring microscopic features. Adv. Mater. Interfaces *5*, 1800403.

Peng, X., Dong, K., Ye, C., Jiang, Y., Zhai, S., Cheng, R., Liu, D., Gao, X., Wang, J., and Wang, Z.L. (2020). A breathable, biodegradable, antibacterial, and self-powered electronic skin based on all-nanofiber triboelectric nanogenerators. Sci. Adv. *6*, eaba9624.

Peng, X., Dong, K., Ning, C.A., Cheng, R.W., Yi, J., Zhang, Y.H., Sheng, F.F., Wu, Z.Y., and Wang, Z.L. (2021). All-nanofiber self-powered skin-interfaced real-time respiratory monitoring system for obstructive sleep apnea-hypopnea syndrome diagnosing. Adv. Funct. Mater. *31*, 2103559.

Petritz, A., Karner-Petritz, E., Uemura, T., Schaffner, P., Araki, T., Stadlober, B., and Sekitani, T. (2021). Imperceptible energy harvesting device and biomedical sensor based on ultraflexible ferroelectric transducers and organic diodes. Nat. Commun. *12*, 2399.

Pyo, S., Lee, J., Bae, K., Sim, S., and Kim, J. (2021). Recent progress in flexible tactile sensors for human-interactive systems: from sensors to advanced applications. Adv. Mater. *33*, e2005902.

Ruth, S.R.A., Feig, V.R., Tran, H., and Bao, Z.N. (2020). Microengineering pressure sensor active layers for improved performance. Adv. Funct. Mater. *30*, 2003491.

Sencadas, V., Tawk, C., Searle, T., and Alici, G. (2021). Low-hysteresis and ultrasensitive microcellular structures for wearable electronic applications. ACS Appl. Mater. Interfaces *13*, 1632–1643.

Sharma, S., Chhetry, A., Zhang, S., Yoon, H., Park, C., Kim, H., Sharifuzzaman, M., Hui, X., and Park, J.Y. (2021). Hydrogen-bond-triggered hybrid nanofibrous membrane-based wearable pressure sensor with ultrahigh sensitivity over a broad pressure range. ACS Nano *15*, 4380–4393.

Shi, J., Wang, L., Dai, Z., Zhao, L., Du, M., Li, H., and Fang, Y. (2018). Multiscale hierarchical design of a flexible piezoresistive pressure sensor with high sensitivity and wide linearity range. Small *14*, e1800819.

Song, Z., Li, W., Bao, Y., Wang, W., Liu, Z., Han, F., Han, D., and Niu, L. (2018). Bioinspired microstructured pressure sensor based on a janus graphene film for monitoring vital signs and cardiovascular assessment. Adv. Electron. Mater. *4*, 1800252.

Sun, L.J., Chen, S., Guo, Y.F., Song, J.C., Zhang, L.Z., Xiao, L.J., Guan, Q.B., and You, Z.W. (2019). Ionogel-based, highly stretchable, transparent, durable triboelectric nanogenerators for energy harvesting and motion sensing over a wide temperature range. Nano Energy *63*, 103847.

Syu, M.H., Guan, Y.J., Lo, W.C., and Fuh, Y.K. (2020). Biomimetic and porous nanofiber-based hybrid sensor for multifunctional pressure sensing and human gesture identification via deep learning method. Nano Energy *76*, 105029.

Tan, C., Dong, Z., Li, Y., Zhao, H., Huang, X., Zhou, Z., Jiang, J.-W., Long, Y.-Z., Jiang, P., Zhang, T.-Y., and Sun, B. (2020). A high performance wearable strain sensor with advanced thermal management for motion monitoring. Nat. Commun. *11*, 3530.

Tang, X., Wu, C., Gan, L., Zhang, T., Zhou, T., Huang, J., Wang, H., Xie, C., and Zeng, D. (2019). Multilevel microstructured flexible pressure sensors with ultrahigh sensitivity and ultrawide pressure range for versatile electronic skins. Small *15*, e1804559.

Tang, X., Yang, W., Yin, S., Tai, G., Su, M., Yang, J., Shi, H., Wei, D., and Yang, J. (2021). Controllable graphene wrinkle for a high-performance flexible pressure sensor. ACS Appl. Mater. Interfaces *13*, 20448–20458.

Tian, K., Sui, G., Yang, P., Deng, H., and Fu, Q. (2020). Ultrasensitive thin-film pressure sensors with a broad dynamic response range and excellent versatility toward pressure, vibration, bending, and temperature. ACS Appl. Mater. Interfaces *12*, 20998–21008.

Wang, Z., Guan, X., Huang, H., Wang, H., Lin, W., and Peng, Z. (2019). Full 3D printing of stretchable piezoresistive sensor with hierarchical porosity and multimodulus architecture. Adv. Funct. Mater. *29*, 1807569.

Wang, H., Cen, Y., and Zeng, X. (2021a). Highly sensitive flexible tactile sensor mimicking the microstructure perception behavior of human skin. ACS Appl. Mater. Interfaces *13*, 28538–28545.

Wang, J., He, J., Ma, L., Yao, Y., Zhu, X., Peng, L., Liu, X., Li, K., and Qu, M. (2021b). A humidity-resistant, stretchable and wearable textile-based triboelectric nanogenerator for mechanical energy harvesting and multifunctional self-powered haptic sensing. Chem. Eng. J. *423*, 130200.

Wang, L., Huang, X., Wang, D., Zhang, W., Gao, S., Luo, J., Guo, Z., Xue, H., and Gao, J. (2021c). Lotus leaf inspired superhydrophobic rubber composites for temperature stable piezoresistive sensors with ultrahigh compressibility and linear working range. Chem. Eng. J. *405*, 127025.

Wang, S., Chen, G., Yao, B., Chee, A.J.Y., Wang, Z., Du, P., Qu, S., and Yu, A.C.H. (2021d). In situ and intraoperative detection of the ureter injury using a highly sensitive piezoresistive sensor with

a tunable porous structure. ACS Appl. Mater. Interfaces *13*, 21669–21679.

Wu, Q., Qiao, Y., Guo, R., Naveed, S., Hirtz, T., Li, X., Fu, Y., Wei, Y., Deng, G., Yang, Y., et al. (2020a). Triode-mimicking graphene pressure sensor with positive resistance variation for physiology and motion monitoring. ACS Nano *14*, 10104–10114.

Wu, X., Khan, Y., Ting, J., Zhu, J., Ono, S., Zhang, X., Du, S., Evans, J.W., Lu, C., and Arias, A.C. (2020b). Large-area fabrication of high-performance flexible and wearable pressure sensors. Adv. Electron. Mater. *6*, 1901310.

Wu, J., Pang, H., Ding, L., Wang, Y., He, X., Shu, Q., Xuan, S., and Gong, X. (2021). A lightweight, ultrathin aramid-based flexible sensor using a combined inkjet printing and buckling strategy. Chem. Eng. J. *421*, 129830.

Xiang, Y., Fang, L., Wu, F., Zhang, S., Ruan, H., Luo, H., Zhang, H., Li, W., Long, X., Hu, B., and Zhou, M. (2021). 3D crinkled ALK-Ti_3C_2 MXene based flexible piezoresistive sensors with ultra-high sensitivity and ultra-wide pressure range. Adv. Mater. Technol. *6*, 2001157.

Xiong, Y., Shen, Y., Tian, L., Hu, Y., Zhu, P., Sun, R., and Wong, C.-P. (2020a). A flexible, ultra-highly sensitive and stable capacitive pressure sensor with convex microarrays for motion and health monitoring. Nano Energy *70*, 104436.

Xiong, Y., Zhu, Y., Liu, X., Zhu, P., Hu, Y., Sun, R., and Wong, C.-P. (2020b). A flexible pressure sensor based on melamine foam capped by copper nanowires and reduced graphene oxide. Mater. Today Commun. *24*, 100970.

Xu, L., Zhang, Z., Gao, F., Zhao, X., Xun, X., Kang, Z., Liao, Q., and Zhang, Y. (2021). Self-powered ultrasensitive pulse sensors for noninvasive multi-indicators cardiovascular monitoring. Nano Energy *81*, 105614.

Yang, J.Y., Tang, D., Ao, J.P., Ghosh, T., Neumann, T.V., Zhang, D.G., Piskarev, Y., Yu, T.T., Truong, V.K., Xie, K., et al. (2020). Ultrasoft liquid metal elastomer foams with positive and negative piezopermittivity for tactile sensing. Adv. Funct. Mater. *30*, 2002611.

Yang, J., Liu, Q., Deng, Z., Gong, M., Lei, F., Zhang, J., Zhang, X., Wang, Q., Liu, Y., Wu, Z., and Guo, C.F. (2019a). Ionic liquid–activated wearable electronics. Mater. Today Phys. *8*, 78–85.

Yang, J.C., Kim, J.O., Oh, J., Kwon, S.Y., Sim, J.Y., Kim, D.W., Choi, H.B., and Park, S. (2019b). Microstructured porous pyramid-based ultrahigh sensitive pressure sensor insensitive to strain and temperature. ACS Appl. Mater. Interfaces *11*, 19472–19480.

Yang, C., Huang, X., Li, X., Yang, C., Zhang, T., Wu, Q., Liu, D., Lin, H., Chen, W., Hu, N., and Xie, X. (2021a). Wearable and implantable intraocular pressure biosensors: recent progress and future prospects. Adv. Sci. *8*, 2002971.

Yang, T., Deng, W., Chu, X., Wang, X., Hu, Y., Fan, X., Song, J., Gao, Y., Zhang, B., Tian, G., et al. (2021b). Hierarchically microstructure-bioinspired flexible piezoresistive bioelectronics. ACS Nano. *15*, 11555–11563.

Yao, H., Yang, W., Cheng, W., Tan, Y.J., See, H.H., Li, S., Ali, H.P.A., Lim, B.Z.H., Liu, Z., and Tee, B.C.K. (2020). Near–hysteresis-free soft tactile electronic skins for wearables and reliable machine learning. Proc. Natl. Acad. Sci. U S A *117*, 25352–25359.

Yi, C., Hou, Y., He, K., Li, W., Li, N., Wang, Z., Yang, B., Xu, S., Wang, H., Gao, C., et al. (2020). Highly sensitive and wide linear-response pressure sensors featuring zero standby power consumption under bending conditions. ACS Appl. Mater. Interfaces *12*, 19563–19571.

Yin, J., Hinchet, R., Shea, H., and Majidi, C. (2021a). Wearable soft technologies for haptic sensing and feedback. Adv. Funct. Mater. *31*, 2007428.

Yin, R.Y., Wang, D.P., Zhao, S.F., Lou, Z., and Shen, G.Z. (2021b). Wearable sensors-enabled human-machine interaction systems: from design to application. Adv. Funct. Mater. *31*, 2008936.

Yin, Y.M., Li, H.Y., Xu, J., Zhang, C., Liang, F., Li, X., Jiang, Y., Cao, J.W., Feng, H.F., Mao, J.N., et al. (2021c). Facile fabrication of flexible pressure sensor with programmable lattice structure. ACS Appl. Mater. Interfaces *13*, 10388–10396.

Yu, Y., Zheng, G., Dai, K., Zhai, W., Zhou, K., Jia, Y., Zheng, G., Zhang, Z., Liu, C., and Shen, C. (2021). Hollow-porous fibers for intrinsically thermally insulating textiles and wearable electronics with ultrahigh working sensitivity. Mater. Horiz. *8*, 1037–1046.

Zhang, J.H., Li, Y., Du, J.H., Hao, X.H., and Wang, Q. (2019a). Bio-inspired hydrophobic/cancellous/hydrophilic trimurti PVDF mat-based wearable triboelectric nanogenerator designed by self-assembly of electro-pore-creating. Nano Energy *61*, 486–495.

Zhang, T., Li, Z., Li, K., and Yang, X. (2019b). Flexible pressure sensors with wide linearity range and high sensitivity based on selective laser sintering 3D printing. Adv. Mater. Technol. *4*, 1900679.

Zhang, S., Sun, K., Liu, H., Chen, X., Zheng, Y., Shi, X., Zhang, D., Mi, L., Liu, C., and Shen, C. (2020a). Enhanced piezoresistive performance of conductive WPU/CNT composite foam through incorporating brittle cellulose nanocrystal. Chem. Eng. J. *387*, 124045.

Zhang, W., Xiao, Y., Duan, Y., Li, N., Wu, L., Lou, Y., Wang, H., and Peng, Z. (2020b). A high-performance flexible pressure sensor realized by overhanging cobweb-like structure on a micropost array. ACS Appl. Mater. Interfaces *12*, 48938–48947.

Zhang, Y., Zhao, Y., Zhai, W., Zheng, G., Ji, Y., Dai, K., Mi, L., Zhang, D., Liu, C., and Shen, C. (2021a). Multifunctional interlocked e-skin based on elastic micropattern array facilely prepared by hot-air-gun. Chem. Eng. J. *407*, 127960.

Zhang, Z.A., Gui, X.C., Hu, Q.M., Yang, L.L., Yang, R.L., Huang, B.F., Yang, B.R., and Tang, Z.K. (2021b). Highly sensitive capacitive pressure sensor based on a micropyramid array for health and motion monitoring. Adv. Electron. Mater. *7*, 2100174.

Zhao, T., Yuan, L., Li, T., Chen, L., Li, X., and Zhang, J. (2020). Pollen-shaped hierarchical structure for pressure sensors with high sensitivity in an ultrabroad linear response range. ACS Appl. Mater. Interfaces *12*, 55362–55371.

Zhao, H., Zhou, Y., Cao, S., Wang, Y., Zhang, J., Feng, S., Wang, J., Li, D., and Kong, D. (2021a). Ultrastretchable and washable conductive microtextiles by coassembly of silver nanowires and elastomeric microfibers for epidermal human–machine interfaces. ACS Mater. Lett. *3*, 912–920.

Zhao, L.J., Wang, L.L., Zheng, Y.Q., Zhao, S.F., Wei, W., Zhang, D.W., Fu, X.Y., Jiang, K., Shen, G.Z., and Han, W. (2021b). Highly-stable polymer-crosslinked 2D MXene-based flexible biocompatible electronic skins for in vivo biomonitoring. Nano Energy *84*, 105921.

Zheng, Q., Lee, J.-h., Shen, X., Chen, X., and Kim, J.-K. (2020). Graphene-based wearable piezoresistive physical sensors. Mater. Today *36*, 158–179.

Zheng, Y., Lin, T., Zhao, N., Huang, C., Chen, W., Xue, G., Wang, Y., Teng, C., Wang, X., and Zhou, D. (2021). Highly sensitive electronic skin with a linear response based on the strategy of controlling the contact area. Nano Energy *85*, 106013.

Zhong, M.J., Zhang, L.J., Liu, X., Zhou, Y.N., Zhang, M.Y., Wang, Y.J., Yang, L., and Wei, D. (2021). Wide linear range and highly sensitive flexible pressure sensor based on multistage sensing process for health monitoring and human-machine interfaces. Chem. Eng. J. *412*, 128649.

Zhou, K., Zhang, C., Xiong, Z.Y., Chen, H.Y., Li, T., Ding, G.L., Yang, B.D., Liao, Q.F., Zhou, Y., and Han, S.T. (2020a). Template-directed growth of hierarchical MOF hybrid arrays for tactile sensor. Adv. Funct. Mater. *30*, 2001296.

Zhou, K.K., Zhao, Y., Sun, X.P., Yuan, Z.Q., Zheng, G.Q., Dai, K., Mi, L.W., Pan, C.F., Liu, C.T., and Shen, C.Y. (2020b). Ultra-stretchable triboelectric nanogenerator as high-sensitive and self-powered electronic skins for energy harvesting and tactile sensing. Nano Energy *70*, 104546.

Zhu, G.J., Ren, P.G., Wang, J., Duan, Q., Ren, F., Xia, W.M., and Yan, D.X. (2020). A highly sensitive and broad-range pressure sensor based on polyurethane mesodome arrays embedded with silver nanowires. ACS Appl. Mater. Interfaces *12*, 19988–19999.

Zou, B., Chen, Y., Liu, Y., Xie, R., Du, Q., Zhang, T., Shen, Y., Zheng, B., Li, S., Wu, J., et al. (2019). Repurposed leather with sensing capabilities for multifunctional electronic skin. Adv. Sci. *6*, 1801283.